



**HAL**  
open science

## Gain-of-function and loss-of-function variants in GRIA3 lead to distinct neurodevelopmental phenotypes

Berardo Rinaldi, Allan Bayat, Linda Zachariassen, Jia-Hui Sun, Yu-Han Ge, Dan Zhao, Kristine Bonde, Laura Madsen, Ilham Abdimunim Ali Awad, Duygu Bagiran, et al.

### ► To cite this version:

Berardo Rinaldi, Allan Bayat, Linda Zachariassen, Jia-Hui Sun, Yu-Han Ge, et al.. Gain-of-function and loss-of-function variants in GRIA3 lead to distinct neurodevelopmental phenotypes. *Brain - A Journal of Neurology* , 2023, 10.1093/brain/awad403 . hal-04386909

HAL Id: hal-04386909

<https://univ-rennes.hal.science/hal-04386909v1>

Submitted on 15 Feb 2024

**HAL** is a multi-disciplinary open access archive for the deposit and dissemination of scientific research documents, whether they are published or not. The documents may come from teaching and research institutions in France or abroad, or from public or private research centers.

L'archive ouverte pluridisciplinaire **HAL**, est destinée au dépôt et à la diffusion de documents scientifiques de niveau recherche, publiés ou non, émanant des établissements d'enseignement et de recherche français ou étrangers, des laboratoires publics ou privés.



Distributed under a Creative Commons Attribution - NonCommercial 4.0 International License

# Gain-of-function and loss-of-function variants in *GRIA3* lead to distinct neurodevelopmental phenotypes

Berardo Rinaldi,<sup>1,†</sup> Allan Bayat,<sup>2,3,4,†</sup> Linda G. Zachariassen,<sup>2,†</sup> Jia-Hui Sun,<sup>5,6,†</sup> Yu-Han Ge,<sup>5,7</sup>  
Dan Zhao,<sup>2</sup> Kristine Bonde,<sup>2</sup> Laura H. Madsen,<sup>2</sup> Ilham Abdimunim Ali Awad,<sup>2</sup> Duygu Bagiran,<sup>2</sup>  
Amal Sbeih,<sup>2</sup> Syeda Maidah Shah,<sup>2</sup> Shaymaa El-Sayed,<sup>2</sup> Signe M. Lyngby,<sup>2</sup> Miriam G.  
Pedersen,<sup>2</sup> Charlotte Stenum-Berg,<sup>2</sup> Louise Claudia Walker,<sup>8</sup> Ilona Krey,<sup>9</sup> Andrée Delahaye-  
Duriez,<sup>10,11,12</sup> Lisa T. Emrick,<sup>13,14</sup> Krystal Sully,<sup>13</sup> Chaya N. Murali,<sup>14</sup> Lindsay C. Burrage,<sup>14</sup> Julie  
Ana Plaud Gonzalez,<sup>13</sup> Mered Parnes,<sup>13,15</sup> Jennifer Friedman,<sup>16,17,18</sup> Bertrand Isidor,<sup>19</sup> Jérémie  
Lefranc,<sup>20</sup> Sylvia Redon,<sup>21,22</sup> Delphine Heron,<sup>23,24</sup> Cyril Mignot,<sup>23,24</sup> Boris Keren,<sup>25</sup> Mélanie  
Fradin,<sup>26</sup> Christele Dubourg,<sup>27,28</sup> Sandra Mercier,<sup>29,30</sup> Thomas Besnard,<sup>29,30</sup> Benjamin Cogne,<sup>29,30</sup>  
Wallid Deb,<sup>29,30</sup> Clotilde Rivier,<sup>31</sup> Donatella Milani,<sup>32</sup> Maria Francesca Bedeschi,<sup>1</sup> Claudia Di  
Napoli,<sup>1</sup> Federico Grilli,<sup>1</sup> Paola Marchisio,<sup>33,34</sup> Suzanna Koudijs,<sup>35</sup> Danielle Veenma,<sup>35</sup> Emanuela  
Argilli,<sup>37,38</sup> Sally Ann Lynch,<sup>39</sup> Ping Yee Billie Au,<sup>40</sup> Fernando Eduardo Ayala Valenzuela,<sup>41</sup>  
Carolyn Brown,<sup>42</sup> Diane Masser-Frye,<sup>43</sup> Marilyn Jones,<sup>44</sup> Leslie Patron Romero,<sup>45</sup> Wenhui Laura  
Li,<sup>46</sup> Erin Thorpe,<sup>42</sup> Laura Hecher,<sup>46</sup> Jessika Johannsen,<sup>46</sup> Jonas Denecke,<sup>46</sup> Vanda McNiven,<sup>47,48</sup>  
Anna Szuto,<sup>47,49</sup> Emma Wakeling,<sup>50</sup> Vincent Cruz,<sup>51</sup> Valerie Sency,<sup>51</sup> Heng Wang,<sup>51</sup> Juliette  
Piard,<sup>52,53</sup> Fanny Kortüm,<sup>54</sup> Theresia Herget,<sup>54</sup> Tatjana Bierhals,<sup>54</sup> Angelo Condell,<sup>55</sup> Bruria Ben  
Zeev,<sup>56,57</sup> Simranpreet Kaur,<sup>55,58</sup> John Christodoulou,<sup>55,58,59,60</sup> Amelie Piton,<sup>61</sup> Christiane  
Zweier,<sup>62,63</sup> Cornelia Kraus,<sup>62</sup> Alessia Micalizzi,<sup>64</sup> Marina Trivisano,<sup>65</sup> Nicola Specchio,<sup>65</sup> Gaetan  
Lesca,<sup>66,67</sup> Rikke S. Møller,<sup>3,4</sup> Zeynep Tümer,<sup>68,69</sup> Maria Musgaard,<sup>8</sup> Benedicte Gerard,<sup>70</sup>  
Johannes R. Lemke,<sup>71</sup> Yun Stone Shi<sup>5,7,72</sup> and Anders S. Kristensen<sup>2</sup>

<sup>†</sup>These authors contributed equally to this work.

## Abstract

AMPA ( $\alpha$ -amino-3-hydroxy-5-methyl-4-isoxazole propionic acid) receptors (AMPA receptors) mediate fast excitatory neurotransmission in the brain. AMPARs form by homo- or heteromeric assembly of subunits encoded by the *GRIA1-GRIA4* genes, of which only *GRIA3* is X-chromosomal.

1 Increasing numbers of *GRIA3* missense variants are reported in patients with  
2 neurodevelopmental disorders (NDD), but only a few have been examined functionally.

3 Here, we evaluated the impact on AMPAR function of one frameshift and 43 rare missense  
4 *GRIA3* variants identified in patients with NDD by electrophysiological assays. Thirty-one  
5 variants alter receptor function and show loss-of-function (LoF) or gain-of-function (GoF)  
6 properties, whereas 13 appeared neutral.

7 We collected detailed clinical data from 25 patients (from 23 families) harbouring 17 of these  
8 variants. All patients had global developmental impairment, mostly moderate (9/25) or severe  
9 (12/25). Twelve patients had seizures, including focal motor (6/12), unknown onset motor (4/12),  
10 focal impaired awareness (1/12), (atypical) absence (2/12), myoclonic (5/12), and generalized  
11 tonic-clonic (1/12) or atonic (1/12) seizures. The epilepsy syndrome was classified as  
12 developmental and epileptic encephalopathy in eight patients, developmental encephalopathy  
13 without seizures in 13 patients, and intellectual disability with epilepsy in four patients. Limb  
14 muscular hypotonia was reported in 13/25, and hypertonia in 10/25. Movement disorders were  
15 reported in 14/25, with hyperekplexia or non-epileptic erratic myoclonus being the most  
16 prevalent feature (8/25).

17 Correlating receptor functional phenotype with clinical features revealed clinical features for  
18 *GRIA3*-associated NDDs and distinct NDD phenotypes for LoF and GoF variants. GoF variants  
19 were associated with more severe outcomes: patients were younger at the time of seizure onset  
20 (median age one month), hypertonic, and more often had movement disorders, including  
21 hyperekplexia. Patients with LoF variants were older at the time of seizure onset (median age 16  
22 months), hypotonic, and had sleeping disturbances. LoF and GoF variants were disease-causing  
23 in both sexes but affected males often carried *de novo* or hemizygous LoF variants inherited  
24 from healthy mothers, whereas all but one affected females had *de novo* heterozygous GoF  
25 variants.

26

27 **Author affiliations:**

28 1 Medical Genetics Unit, Fondazione IRCCS Ca' Granda Ospedale Maggiore Policlinico, Milan,  
29 20122, Italy

1 2 Department of Drug Design and Pharmacology, University of Copenhagen, Copenhagen, 2100,  
2 Denmark

3 3 Department of Epilepsy Genetics and Personalized Medicine, Danish Epilepsy Centre,  
4 Dianalund, 4293, Denmark

5 4 Department of Regional Health Research, University of Southern Denmark, Odense, 5230  
6 Denmark

7 5 State Key Laboratory of Pharmaceutical Biotechnology, Model Animal Research Center,  
8 Department of Neurology, Nanjing Drum Tower Hospital, Medical School, Nanjing University,  
9 Nanjing, 210032, China

10 6 Zhejiang Key Laboratory of Organ Development and Regeneration, College of Life and  
11 Environmental Sciences, Hangzhou Normal University, Hangzhou, 310030 ,China

12 7 Ministry of Education Key Laboratory of Model Animal for Disease Study, National Resource  
13 Center for Mutant Mice, Jiangsu Key Laboratory of Molecular Medicine, Medical School,  
14 Nanjing University, Nanjing, 210032, China

15 8 Department of Chemistry and Biomolecular Sciences, University of Ottawa, Ottawa, K1H  
16 8M5, Canada

17 9 Institute of Human Genetics, University of Leipzig Medical Center, Leipzig, 04103, Germany

18 10 Unité fonctionnelle de médecine génomique et génétique clinique, Hôpital Jean Verdier,  
19 Assistance Publique des Hôpitaux de Paris, Bondy, 93140, France

20 11 NeuroDiderot, UMR 1141, Inserm, Université Paris Cité, Paris, 75019, France

21 12 UFR SMBH, Université Sorbonne Paris Nord, Bobigny, 93000, France

22 13 Division of Neurology and Developmental Neurosciences, Department of Pediatrics, Baylor  
23 College of Medicine, Texas Children's Hospital, Houston, Texas, 77030, USA

24 14 Department of Molecular and Human Genetics, Baylor College of Medicine, Houston, Texas,  
25 77030, USA

26 15 Pediatric Movement Disorders Clinic, Texas Children's Hospital and Baylor College of  
27 Medicine, Houston, Texas, 77030, USA

- 1 16 Rady Children's Institute for Genomic Medicine, San Diego, California, 92123, USA
- 2 17 Department of Neurosciences, University of California San Diego, San Diego, CA 92123,  
3 USA
- 4 18 Department of Pediatrics, University of California San Diego, San Diego, CA 92123, USA
- 5 19 Service de Génétique Médicale, Centre Hospitalier Universitaire de Nantes, Nantes, Pays de  
6 la Loire, 44000, France
- 7 20 Pediatric Neurophysiology Department, CHU de Brest, Brest, 29200, France
- 8 21 Service de Génétique Médicale, CHU de Brest, Brest, 29200, France
- 9 22 University of Brest, Inserm, EFS, UMR 1078, GGB, Brest, 29200, France
- 10 23 APHP Sorbonne Université, Département de Génétique, Hôpital Armand Trousseau and  
11 Groupe Hospitalier Pitié-Salpêtrière, Paris, 75013, France
- 12 24 Centre de Référence Déficiences Intellectuelles de Causes Rares, Paris, 75013, France
- 13 25 Genetic Department, APHP, Sorbonne Université, Pitié-Salpêtrière Hospital, Paris, 75013,  
14 France
- 15 26 Service de Génétique Médicale, Hôpital Sud, CHU de Rennes, Rennes, 35200, France
- 16 27 Service de Génétique Moléculaire et Génomique, CHU de Rennes, Rennes, 35200, France
- 17 28 Université de Rennes, CNRS, Institut de Genetique et Developpement de Rennes, UMR  
18 6290, Rennes, 35200, France
- 19 29 Nantes Université, CHU Nantes, Service de Génétique Médicale, Nantes, 44000, France
- 20 30 Nantes Université, CHU Nantes, CNRS, INSERM, l'institut du thorax, Nantes, 44000, France
- 21 31 Department of Paediatrics, Villefranche-sur-Saône Hospital, Villefranche-sur-Saône , 69655,  
22 France
- 23 32 Fondazione IRCCS Ca' Granda Ospedale Maggiore Policlinico, Milan, 20122, Italy
- 24 33 Fondazione IRCCS Ca' Granda Ospedale Maggiore Policlinico, Pediatria  
25 Pneumoinfettivologia, Milan, 20122, Italy
- 26 34 University of Milan, Milan, 20122, Italy

1 35 Department of Neurology, ENCORE, Erasmus Medical Center-Sophia Children's Hospital,  
2 Rotterdam, 3015, The Netherlands

3 36 Department of Pediatrics, ENCORE, Erasmus Medical Center-Sophia Children's Hospital,  
4 Rotterdam, 3015, The Netherlands

5 37 Institute of Human Genetics, University of California, San Francisco, CA 94143, USA

6 38 Department of Neurology, Weill Institute for Neurosciences, University of California, San  
7 Francisco, CA 94143, USA

8 39 Department of Clinical Genetics Children's Health Ireland Crumlin, Dublin, D12 N512,  
9 Ireland

10 40 Department of Medical Genetics, Alberta Children's Hospital Research Institute, Cumming  
11 School of Medicine, University of Calgary, Calgary, AB T2N 4N1, Canada

12 41 Hospital Angeles Tijuana, Tijuana, 22010, Mexico

13 42 Illumina Inc, San Diego, California, 92122, USA

14 43 Division of Genetics, Department of Pediatrics, UC San Diego School of Medicine, Rady  
15 Children's Hospital, San Diego, California, 92024, USA

16 44 Facultad de Medicina y Psicología, Universidad Autónoma de Baja California, Tijuana,  
17 22010, Mexico

18 45 Breakthrough Genomics Inc, Irvine, California, 92618, USA

19 46 Department of Pediatrics, University Medical Center Hamburg-Eppendorf, Hamburg, 20215,  
20 Germany

21 47 Division of Clinical and Metabolic Genetics, The Hospital for Sick Children, University of  
22 Toronto, Toronto, Ontario, ON M5G 1E8, Canada

23 48 Fred A Litwin Family Centre in Genetic Medicine, University Health Network and Mount  
24 Sinai Hospital, Toronto, Ontario, ON M5G 2C4, Canada

25 49 Department of Paediatrics, Hospital for Sick Children and University of Toronto, Toronto,  
26 ON M5G 1E8, Canada

1 50 North East Thames Regional Genetics Service, Great Ormond Street Hospital for Children  
2 NHS Foundation Trust, London, WC1N 3JH, UK

3 51 DDC Clinic Center for Special Needs Children, Middlefield, Ohio, 44062, USA

4 52 Centre de Génétique Humaine, Université de Franche-Comté, CHU, Besançon, 25000, France

5 53 Unité de recherche en neurosciences intégratives et cognitives EA481, Université de Franche-  
6 Comté, Besançon, 25000, France

7 54 Institute of Human Genetics, University Medical Center Hamburg-Eppendorf, Hamburg,  
8 20251, Germany

9 55 Brain and Mitochondrial Research Group, Murdoch Children's Research Institute,  
10 Melbourne, Victoria, 3052, Australia

11 56 Pediatric Neurology Institute, Edmond and Lily Safra Children's Hospital, Sheba Medical  
12 Center, Tel HaShomer, Ramat Gan, 52621, Israel

13 57 Sackler School of Medicine, Tel Aviv University, Tel-Aviv, 69978, Israel

14 58 Department of Paediatrics, Melbourne Medical School, University of Melbourne, Melbourne,  
15 Victoria, 3052, Australia

16 59 Discipline of Genetic Medicine, Sydney Medical School, University of Sydney, Sydney, New  
17 South Wales, 2050, Australia

18 60 Discipline of Child & Adolescent Health, Sydney Medical School, University of Sydney,  
19 Sydney, New South Wales, 2050, Australia

20 61 Hôpitaux Universitaires de Strasbourg, Laboratoire de Diagnostic Génétique, Strasbourg,  
21 67000, France

22 62 Institute of Human Genetics, Friedrich-Alexander-Universität Erlangen-Nürnberg, Erlangen,  
23 91054, Germany

24 63 Department of Human Genetics, Inselspital Bern, University of Bern, Bern, 3010,  
25 Switzerland

26 64 Translational Cytogenomics Research Unit, Bambino Gesù Children's Hospital, IRCCS,  
27 Rome, 00165, Italy

1 65 Neurology, Epilepsy and Movement Disorders, Bambino Gesù Children's Hospital, IRCCS,  
2 Full Member of European Reference Network EpiCARE, Rome, 00165, Italy

3 66 Department of Medical Genetics, University Hospital of Lyon and Claude Bernard Lyon I  
4 University, Lyon, 69100, France

5 67 Pathophysiology and Genetics of Neuron and Muscle (PNMG), UCBL, CNRS UMR5261 -  
6 INSERM U1315, Lyon, 69100, France

7 68 Kennedy Center, Department of Clinical Genetics, Copenhagen University Hospital,  
8 Rigshospitalet, Copenhagen, Denmark

9 69 Department of Clinical Medicine, Faculty of Health and Medical Sciences, University of  
10 Copenhagen, Copenhagen, 2100, Denmark

11 70 Laboratoires de diagnostic genetique, Institut de genetique Medicale d'Alsace, Hopitaux  
12 Universitaires de Strasbourg, Strasbourg, 67000, France

13 71 Center for Rare Diseases, University of Leipzig Medical Center, Leipzig, 04103, Germany

14 72 Guangdong Institute of Intelligence Science and Technology, Zhuhai, 519031, China

15

16 Correspondence to: Allan Bayat, MD (clinical data)

17 Department of Epilepsy Genetics and Personalized Medicine, Danish Epilepsy Centre,  
18 Dianalund, Denmark

19 E-mail: [abaya@filadelfia.dk](mailto:abaya@filadelfia.dk)

20

21 Correspondence may also be addressed to: Yun Stone Shi, PhD (functional evaluation)

22 Department of Neurology, Nanjing University, Nanjing, China

23 E-mail: [yunshi@nju.edu.cn](mailto:yunshi@nju.edu.cn)

24

25 Anders Skov Kristensen, PhD (functional evaluation)



1 Department of Drug Design and Pharmacology, University of Copenhagen, Copenhagen,  
2 Denmark

3 E-mail: ask@sund.ku.dk

4

5 **Running title:** Evaluation of *GRIA3* variants

6

7 **Keywords:** AMPA receptor; GRIA; GRIA3; clinical biomarker; genotype-phenotype

8 **Abbreviations:** agonist binding domain = ABD;  $\alpha$ -amino-3-hydroxy-5-methyl-4-  
9 isoxazolepropionic acid = AMPA; Dulbecco's modified Eagle's medium = DMEM; glutamate =  
10 Glu; ionotropic glutamate receptors = iGluR; kainic acid = KA; neurodevelopment disorders =  
11 NDDs; N-terminal domain = NTD; whole exome sequencing = WES; two-electrode voltage-  
12 clamp = TEVC; transmembrane domain = TMD; C-terminal domain (CTD)

13

14 Correspondence to: Allan Bayat, MD (clinical data)

15 Department of Epilepsy Genetics and Personalized Medicine, Danish Epilepsy Centre,  
16 Dianalund, Denmark

17 E-mail: abaya@filadelfia.dk

18

19 Correspondence may also be addressed to: Yun Stone Shi, PhD (functional evaluation)

20 Department of Neurology, Nanjing University, Nanjing, China

21 E-mail: [yunshi@nju.edu.cn](mailto:yunshi@nju.edu.cn)

22

23 Anders Skov Kristensen, PhD (functional evaluation)

24 Department of Drug Design and Pharmacology, University of Copenhagen, Copenhagen,  
25 Denmark

26 E-mail: ask@sund.ku.dk

1 **Running title:** Evaluation of *GRIA3* variants

2

3 **Keywords:** AMPA receptor; GRIA; GRIA3; clinical biomarker; genotype-phenotype

4 **Abbreviations:** agonist binding domain = ABD;  $\alpha$ -amino-3-hydroxy-5-methyl-4-  
5 isoxazolepropionic acid = AMPA; Dulbecco's modified Eagle's medium = DMEM; glutamate =  
6 Glu; ionotropic glutamate receptors = iGluR; kainic acid = KA; neurodevelopment disorders =  
7 NDDs; N-terminal domain = NTD; whole exome sequencing = WES; two-electrode voltage-  
8 clamp = TEVC; transmembrane domain = TMD; C-terminal domain (CTD)

9

## 10 **Introduction**

11 AMPARs belong to the ionotropic glutamate receptor (iGluR) superfamily of ligand-gated cation  
12 channels<sup>1</sup>. AMPARs are activated by glutamate (Glu) binding, which triggers the transient  
13 opening of a central pore leading to a millisecond influx of cations, denoted excitatory  
14 postsynaptic current (EPSC) that depolarizes the postsynaptic membrane and promotes neuronal  
15 firing<sup>2-4</sup>. AMPAR-mediated EPSCs are essential components in most excitatory glutamatergic  
16 signalling pathways, and normal AMPAR function is critical for most brain functions, including  
17 learning and memory formation<sup>5-13</sup>. The assembly of GluA1-A4 subunits into homo- or  
18 heterotetrameric receptor complexes forms diverse subtypes of AMPARs with distinct properties  
19 and expression patterns<sup>14,15</sup>. The GluA1-4 subunit proteins are highly similar and have a modular  
20 architecture of two extracellular domains, the *N*-terminal domain (NTD) and the agonist binding  
21 domain (ABD), a channel-forming transmembrane domain (TMD), and an intracellular carboxy-  
22 terminal domain (CTD) of unknown structure (Fig. 1A). The bilobed ABD of each subunit  
23 contains a single site where Glu binding initiates conformational changes that are transmitted via  
24 semi-flexible linkers to the channel gate in the TMD. Rare genetic variants in the *GRIA1-4*  
25 genes<sup>16-21</sup> may disrupt AMPAR physiology and cause developmental and cognitive impairment,  
26 behavioural, and psychiatric comorbidities, seizures, and cerebral malformations<sup>19,22-56</sup>. *GRIA1*,  
27 *GRIA2*, and *GRIA4* are autosomal genes, whereas *GRIA3* is located on the X-chromosome.  
28 While pathogenic missense variants in *GRIA1*, *GRIA2*, and *GRIA4* appear to arise almost

1 exclusively *de novo*<sup>23,25,28</sup>, pathogenic variants in *GRIA3* may be transmitted from healthy  
2 mothers to affected male children, which is observed in several X-linked NDDs<sup>27,30</sup>.

3 Currently, 20 *GRIA3* missense variants are reported in 30 patients, of whom four are  
4 female<sup>22,26,27,29–35,38,46–49,55</sup>. Of these variants, nine have been functionally tested, revealing or  
5 suggesting loss-of-function (LoF) effects for seven variants detected in fifteen affected males  
6 and in one female<sup>22,29,30,33,35</sup> and gain-of-function (GoF) effects in two variants detected in one  
7 female and one male<sup>32,34</sup>. Thus, the phenotypic and genetic landscape in *GRIA3*-related disorders  
8 remains ill-defined, lacking genotype-phenotype correlations or clinical biomarkers, particularly  
9 in females.

10 We have therefore systematically interrogated the impact on GluA3-containing AMPAR  
11 function of 44 rare inherited or *de novo* *GRIA3* variants identified in patients with NDD to assess  
12 these for pathogenicity and establish LoF or GoF effects for overall receptor signalling function.  
13 Also, for 25 patients with pathogenic LoF or GoF variants, we compared the clinical features  
14 with the functional outcomes to identify genotype-phenotype correlations and clinical  
15 biomarkers that could potentially predict the functional outcome of rare *GRIA3* variants. Our  
16 results show that *GRIA3*-related disorders encompass two patient groups with distinct clinical  
17 features that correlate with the GoF or LoF effect of the variant on receptor function. Also, our  
18 findings expand the general knowledge of the pathogenic contribution of rare genetic alterations  
19 in *GRIA3* to NDDs in the human population with diverse manifestations, influencing both the  
20 timing of disease onset and main clinical symptoms.

21

## 22 **Materials and methods**

### 23 **Materials**

24 Unless otherwise stated, all chemicals were from Sigma-Aldrich (St. Louis, MO). Dulbecco's  
25 modified Eagle's medium (DMEM), fetal bovine serum, trypsin, and penicillin-streptomycin  
26 were from Invitrogen (Carlsbad, CA). DNA modifying enzymes were from New England  
27 Biolabs (Ipswich, MA) except PfuUltra II Fusion HS DNA polymerase (Agilent, Carlsbad, CA).  
28 Cyclothiazide (CTZ), kainic acid, and NASPM were from HelloBio (Bristol, UK).

## 1 **Molecular Biology**

2 *GRIA3* (MIM 138248) variants were introduced by site-directed mutagenesis into their  
3 corresponding positions in cDNA expression constructs encoding GluA3. Specifically, the  
4 plasmid vectors pXOOF and pCAGGS-IRES-EGFP containing cDNA for the unedited GluA3  
5 flip and flop isoforms (GluA3<sub>i</sub> and GluA3<sub>o</sub>, respectively) were used for heterologous expression  
6 in HEK293 cells or generation of mRNA for microinjection in *Xenopus laevis* oocytes (XOs).  
7 For pCAGGS-IRES-EGFP, cDNA for GluA3<sub>i</sub> and GluA3<sub>o</sub> were subcloned into the *NheI* and  
8 *XhoI* restriction sites of the vector. For pXOOF, the cDNA for GluA3<sub>i</sub> was subcloned into the  
9 *EcoRI* and *XhoI* restriction sites. For co-expression with GluA2, GluA2 was subcloned into the  
10 vector pCAGGS-IRES-mCherry. Basepair changes in GluA3 were made by the overlapping PCR  
11 method or the QuickChange mutagenesis kit (Stratagene, La Jolla, CA). Genetic changes were  
12 verified by Sanger DNA sequencing of the entire GluA3 coding region (GATC Biotech,  
13 Constance, Germany). When used as templates for *in vitro* transcription of mRNA, plasmid  
14 constructs were linearized downstream of the 3' untranslated region using the restriction enzyme  
15 *NheI*, column purified using NucleoSpin DNA clean-up kit (Macherey-Nagel, Düren, Germany),  
16 and stored at a concentration of 1.0 µg/µL at -20 °C until use. cRNA transcription was performed  
17 using the ARCA mRNA synthesis kit (NEB, Madison, WI, USA). The resulting mRNA was  
18 purified using the NucleoSpin RNA Clean-up kit (Macherey-Nagel), diluted to 0.5 ng/nL, and  
19 stored at -80 °C until use.

## 21 ***Xenopus laevis* oocyte preparation and injection**

22 Defolliculated XOs (stage V to VI) were prepared and injected with mRNA as described  
23 previously<sup>57</sup>. The care and use of *Xenopus laevis* animals strictly adhered to a protocol (license  
24 2014-15-0201-00031) approved by the Danish Veterinary and Food Administration. Injected  
25 XOs were incubated at 18 °C in Modified Barth's Solution (MBS) containing (in mM) 88 NaCl,  
26 1 KCl, 0.41 CaCl<sub>2</sub>, 2.4 NaHCO<sub>3</sub>, 0.33 Ca(NO<sub>3</sub>)<sub>2</sub>, 0.82 MgSO<sub>4</sub>, 5 Tris (pH 7.4) supplemented  
27 with 50 µg/ml gentamicin until use. For expression of homomeric GluA3 receptors, XOs were  
28 injected with 10 ng cRNA in a volume of 25 nL per oocyte and incubated for 3 days at 18 °C in

1 MBS until the experiment. For expression of heteromeric GluA2/A3 receptors, injection of 10 ng  
2 of a 2:1 mix ratio of GluA2/GluA3 cRNA was used.

3

#### 4 **HEK293 cell culturing and transfection**

5 HEK293T cells were cultured in a 37 °C incubator with 5% CO<sub>2</sub>. Transfection was performed in  
6 35-mm dishes using Lipofectamine2000 reagents (Invitrogen). For co-expression of GluA3 and  
7 GluA2, the ratio of GluA3 to GluA2 cDNA was 1:1. The competitive antagonist NBQX (100  
8 μM) was included in culture media to block receptor-induced cytotoxicity. Twenty-four hours  
9 post-transfection, cells were dissociated with 0.05% trypsin, plated on coverslips pre-treated with  
10 poly-D-lysine, and used for experiments 4 h after plating.

11

#### 12 **Electrophysiology**

13 *Two-electrode voltage-clamp (TEVC) electrophysiology in XOs:* Glass micropipettes (0.69 mm  
14 ID/1.2 mm OD, Harvard Apparatus, Holliston, MA) were pulled on a Sutter P-1000 micropipette  
15 puller (Sutter Instruments, Novato, CA) to a tip resistance of 0.5-2.5 MΩ and filled with 3 M  
16 KCl. Oocytes were clamped using a two-electrode voltage-clamp amplifier (OC-725C, Warner  
17 Instruments, Hamden, CT) and continuously perfused with Frog Ringer's solution containing 115  
18 mM NaCl, 2 mM KCl, 5 mM HEPES, and 1.8 mM BaCl<sub>2</sub> (pH 7.6) by gravity-assisted perfusion  
19 at flow rates of 2 to 4 mL/min into a vertical oocyte flow chamber. Compounds were dissolved  
20 in Frog Ringer's solution and added by bath application. Concentration-response data were  
21 recorded at holding potentials in the -40 to -80 mV range. Each compound solution was applied  
22 for 10 to 60 s depending on the time needed to obtain steady-state currents. Current signals were  
23 low-pass filtered at 5 Hz using an USBPGF-S1 programmable instrumentation low-pass filter  
24 (Alliagator Technologies, Cosa Meda, CA) and digitized with a sampling frequency of 10 Hz  
25 using a CED 1401plus analog-digital converter (Cambridge Electronic Design, Cambridge, UK)  
26 interfaced with a PC running WinWCP software (available from Strathclyde Electrophysiology  
27 Software, University of Strathclyde, Glasgow, UK). Concentration-response experiments were  
28 performed by measuring agonist-evoked current during stepwise application of increasing  
29 concentrations of agonist, as illustrated in Fig. 3E. All experiments were performed at room

1 temperature. *Whole-cell voltage-clamp electrophysiology in HEK293 cells:* The deactivation and  
2 desensitization kinetics of glutamate-evoked currents from WT and mutant GluA3 and GluA2/3  
3 receptors were determined in the whole-cell configuration in HEK293 cells. After the formation  
4 of whole-cell configuration, individual HEK293 cells were lifted with 3 to 5 M $\Omega$  borosilicate  
5 glass pipettes filled with the following internal solution: 135 mM KF, 33 mM KOH, 2 mM  
6 MgCl<sub>2</sub>, 1 mM CaCl<sub>2</sub>, 11 mM EGTA, 10 mM HEPES (pH 7.2). Glu (10 mM) was dissolved in  
7 the extracellular solution: 140 mM NaCl, 2.5 mM KCl, 2 mM CaCl<sub>2</sub>, 1 mM MgCl<sub>2</sub>, 10 mM  
8 HEPES, 5 mM Glucose (pH 7.2). Glutamate pulses of 1 or 500 ms were applied to cells using a  
9 theta-glass pipette mounted on a piezoelectric bimorph driven by gravity. Glutamate-induced  
10 currents were recorded using a MultiClamp 700B amplifier (Axon Instruments) with membrane  
11 potential held at -70 mV. Current signals were recorded with an Axon Digidata 1440 data  
12 acquisition system and with a sampling frequency of 100 kHz following low-pass filtration over  
13 2 kHz. All experiments were performed at room temperature.

14

## 15 **Cohort**

16 Patients with inherited or *de novo* *GRIA3* variants were recruited through an international  
17 collaboration with epilepsy and NDD research groups, the Leipzig GRI-registry  
18 (<https://www.uniklinikum-leipzig.de/einrichtungen/humangenetik/Seiten/GRI-registry.aspx>),  
19 Decipher<sup>58</sup>, ClinVar<sup>59</sup>, and via GeneMatcher<sup>60</sup>. We also contacted the healthcare providers of  
20 previously published patients to collect new or updated clinical information or used that  
21 previously reported in the literature<sup>26,29,33,34,61</sup> (seven patients). Clinical information was  
22 collected by the local physicians or caregivers and included data on the age of seizure onset and  
23 offset, seizure semiology, developmental trajectory, medical history, physical examination, EEG,  
24 and neuroimaging. The study was conducted in agreement with the Declaration of Helsinki. The  
25 Leipzig GRI-registry was approved by the local ethical committee; Leipzig/Germany (224/16-ek  
26 and 379/21-ek). Since all probands were minors or had cognitive impairment, their parents or  
27 legal guardians provided written informed consent.

28

## 1 **Data and statistical analysis**

2 Data for concentration-response curves were obtained from analysis of electrophysiological  
3 recordings of agonist-evoked current responses using ClampFit 10 software (Molecular Devices,  
4 San Jose, CA). Current responses were normalized to the current response by maximal agonist  
5 concentration and used to construct composite concentration-response plots from at least 8  
6 oocytes and fitted using GraphPad Prism v9 (GraphPad Software, San Diego, CA, USA) to a  
7 four-variable Hill equation:

$$8 \quad \text{response} = \text{bottom} + \frac{\text{top} - \text{bottom}}{1 + 10^{(\log EC_{50} - X) \times nH}} \quad (\text{Equation 1})$$

9 where *bottom* is the fitted minimum response, *top* is the fitted maximum response, *nH* is the Hill  
10 slope, *X* is the agonist concentration, and *EC*<sub>50</sub> is the half-maximally effective agonist  
11 concentration, respectively. The time constants for the rate of desensitization ( $\tau_{\text{desens}}$ ) and  
12 deactivation ( $\tau_{\text{deact}}$ ) were obtained by fitting current responses evoked by 500 and 1 ms Glu  
13 pulses with an exponential function using a non-linear least square algorithm (ClampFit):

14

$$15 \quad I = I1 \times \left( \exp\left(-\frac{\text{time}}{\tau1}\right) \right) + I2 \times \left( \exp\left(-\frac{\text{time}}{\tau2}\right) \right) \quad (\text{equation 2})$$

16

17 , where *I* is the total current amplitude, and *I*<sub>1</sub> and *I*<sub>2</sub> are the amplitudes of the fast and slow  
18 current components, respectively, and  $\tau$ <sub>1</sub> and  $\tau$ <sub>2</sub> are the time constants for the decay of the fast  
19 and slow current components. The weighted average  $\tau$  was then calculated as follows:

$$20 \quad \tau_{\text{weighted}} = \left( \frac{I1 \times \tau1 + I2 \times \tau2}{I1 + I2} \right) \quad (\text{equation 3})$$

21 All desensitization time constants were determined using the two-component fitting, and  $\tau_{\text{desens}}$  is  
22 reported as the weighted average  $\tau$ . Except otherwise stated, all deactivation time constants were  
23 determined using mono-exponential fitting, using equation 2 with *I*<sub>2</sub> fixed at 0. Statistical  
24 analyses of data were performed in GraphPad Prism 9. Unless otherwise stated, summary patch-  
25 clamp and TEVC electrophysiology data are represented as mean with a 95% confidence interval  
26 (CI). One-way analysis of variance (ANOVA) with Dunnett's post hoc multiple comparison test  
27 was performed for comparisons of three or more groups in which the data were normally

1 distributed and where a  $P$ -value  $<0.05$  was considered significant. For statistical analysis of  
2 clinical data, quantitative statistics were analyzed using SPSS software (version 24, IBM, United  
3 Kingdom). Two-sided T-test was used to determine the association of clinical features with the  
4 LoF and GoF patient groups.  $P$ -value  $< 0.05$  was considered significant. Unless otherwise stated,  
5 the level of statistical significance is denoted as  $*P < 0.05$ ,  $**P < 0.01$ , and  $***P < 0.001$ .  
6 Extended statistical information including specific  $P$ -values are provided in the Supplementary  
7 information.

8

## 9 **Results**

### 10 ***GRIA3* missense variants in NDD patients concentrate on domains** 11 **responsible for glutamate binding and channel gating**

12 To investigate the pathogenicity of *GRIA3* variants identified in NDD patients, we collected one  
13 frameshift variant and 43 *GRIA3* missense variants identified in patients with presumed *GRIA3*-  
14 related NDD (*Materials and methods*) (Fig. 1, Supplementary table S1). Notably, although the  
15 central elements for channel function (the ABD, TMD, and ABD-TMD linkers) constitute less  
16 than 50% of the GluA3 subunit protein, the majority of the *GRIA3* missense variants are located  
17 in the ABD (15 variants), and TMD (13 variants) domains, and the ABD-TMD linkers (6  
18 variants). In addition, none of these 34/43 variants are reported in the Genome Aggregation  
19 Database (gnomAD), and *GRIA3* is predicted to be constrained to missense variants ( $Z = 4.23$ ),  
20 which indicates intolerance to missense variation, and the majority are predicted to be damaging  
21 by *in silico* prediction of deleteriousness (Supplementary Table S1). In contrast, only 9 variants  
22 affect residues in the NTD and CTD, which are non-critical domains for the core ligand-gated  
23 channel function (Fig. 1A) (Supplementary Table S1).

### 24 ***GRIA3* variants have GoF or LoF effects on GluA3 receptor** 25 **function**

26 The majority of the identified *GRIA3* missense variants have not been functionally evaluated for  
27 effects on GluA3-containing AMPAR function, except for variants p.(Arg450Glu),  
28 p.(Ala615Val), p.(Arg631Ser), p.(Ala653Thr), p.(Arg660Thr), p.(Met706Thr), p.(Glu787Gly),



1 p.(Glu787Lys), p.(Gly826Asp), and p.(Gly833Arg)<sup>22,29,30,32-35</sup>, although not in a systematic  
2 manner. Therefore, we first evaluated all variants with TEVC electrophysiology to directly  
3 compare effects, focusing on key receptor functional features that included current amplitude,  
4 Glu sensitivity, receptor activation, and desensitization properties (Fig. 1B-C). Specifically,  
5 *GRIA3* variants were introduced in cDNA encoding GluA3 and expressed in XOs as homomeric  
6 receptors (*Materials and methods*). We first recorded current responses following the application  
7 of a single high Glu concentration (300  $\mu$ M) with pharmacological blockade of receptor  
8 desensitization (Fig. 1C). Twenty of the variants showed currents that were significantly lower  
9 than WT, including nine variants with undetectable or very small (*e.g.*, 50-fold lower than WT)  
10 current amplitude (Fig. 1B-C; Supplementary Table S2), indicating that these variants have  
11 severe LoF effects on GluA3 subunit function or expression. The single frameshift variant  
12 p.(Gln371Argfs\*6) is located in the 5' end of the NTD-encoding segment of the *GRIA3* coding  
13 sequence (Fig. 1A). Therefore, this variant results in the expression of only the NTD that cannot  
14 form a functional receptor. Indeed, the expression of p.(Gln371Argfs\*6) in XOs did not yield  
15 any current response (Fig. 1C) and is assigned a complete LoF status. The remaining variants  
16 produced current responses with amplitudes similar to or within two-fold range of WT (Fig. 1B  
17 and C; Supplementary Table S2), except for the variants p.(Ala615Val), p.(Ser663Pro), and  
18 p.(Gly803Glu), which showed more than two-fold significantly increased currents compared to  
19 WT, suggesting an overall GoF effect on receptor function.

20 For all functional variants, we performed dose-response experiments with increasing  
21 concentrations of Glu (Fig. 1D), and determined the half-maximally effective concentration  
22 ( $EC_{50}$ ) for receptor activation (Fig. 1E; Supplementary Fig. S2 and Table S3). As summarized in  
23 Fig. 1B, 20 variants changed the  $EC_{50}$  significantly by more than two-fold. The most pronounced  
24 changes were observed for the p.(Ser531Cys), p.(Ala654Thr), p.(Trp799Leu), and p.(Gly803Ala)  
25 variants, which decreased  $EC_{50}$  more than 20-fold (considered a GoF effect), and p.(Met617Thr)  
26 and p.(Phe655Ser), which increased  $EC_{50}$  by more than 20-fold (considered a LoF effect; Fig. 1B  
27 and E, Supplementary Fig. S2, and Table S3).

28 AMPARs undergo profound desensitization in the continued presence of Glu, which is a  
29 key property for EPSC shape and protects against excitotoxicity due to glutamatergic  
30 hyperfunction<sup>62-64</sup>. For variants with a residual function, we assessed potential effects on  
31 receptor desensitization by recording consecutive Glu currents in the absence ( $I_{GLU}$ ) and presence

1 (I<sub>GLU+CTZ</sub>) of CTZ block of desensitization (Fig. 2A). The WT GluA3 receptor showed  
2 desensitized current amplitude of  $2.8 \pm 0.4\%$ ,  $n = 79$ , of the non-desensitized current amplitude  
3 (Fig. 2A-B; Supplementary Table S3); corresponding well with previously reported ratios for  
4 homomeric GluA3<sup>65-67</sup>. Eight variants displayed significant increases in the desensitized current  
5 as illustrated for a representative variant (p.(Ala654Val)) in Fig. 2A. The variants p.(Arg631Ser),  
6 p.(Ala654Pro), p.(Ala654Val), and p.(Ala654Thr) showed the most profound effects, with near  
7 identical current amplitudes under desensitizing and non-desensitizing conditions (Fig. 2A-B;  
8 Supplementary Table S3), which indicate that the variants decrease or fully block receptor  
9 desensitization, which is a GoF effect for AMPAR signalling. In contrast, seven variants  
10 (p.(Ser531Cys), p.(Leu774Ser), p.(Thr776Met), p.(Trp799Leu), p.(Gly803Ala), p.(Thr816Ile),  
11 p.(Gly826Asp)) significantly decreased the desensitized current relative to the non-desensitized  
12 current, indicating an increase in receptor desensitization, which is considered a LoF effect (Fig.  
13 2B; Supplementary Table S3).

14 We screened for changes in the activation properties of GluA3, comparing the receptor  
15 current evoked by application of the weak partial agonist kainic acid (KA) versus the current  
16 evoked by Glu<sup>68,69</sup> (Fig. 2C). When desensitization was blocked, the KA current (I<sub>KA+CTZ</sub>) at WT  
17 GluA3 was  $21 \pm 0.1\%$ ,  $n = 85$ , of the Glu current (Fig. 2B; Supplementary Table S3). The results  
18 from the screening showed an increased KA efficacy for 12 variants (p. (Ala615Val),  
19 p.(Arg631Ser), p.(Ser647Phe), p.(Ala654Prol), p.(Ala654Val), p.(Ala654Thr), p.(Arg660Ser),  
20 p.(Arg660Thr), p.(Ser663Pro), p.(Trp799Leu), p.(Gly803Glu), and p.(Gly803Ala) (Fig. 2C;  
21 Supplementary Table S3). This effect indicates an increase in the ability of GluA3 to translate  
22 agonist binding to channel opening and is to be considered a GoF effect for overall receptor  
23 function. In contrast, six variants (p.(Met617Thr), p.(Ala653Thr), p.(Phe655Ser), p.(Ile665Thr),  
24 p.(Lys701Glu), and p.(Gly826Asp)) displayed decreased KA efficacy, and, therefore, reduced  
25 ability to activate, which is a LoF effect for overall receptor function (Fig. 2B-C; Supplementary  
26 Table S3). Notably, the KA/Glu current ratio has previously been electrophysiologically  
27 characterized for homomeric GluA3 with the p.(Ala653Thr) variant with similar results<sup>29</sup>.

28 Lastly, we screened for constitutive receptor activity, e.g., channel opening in the absence  
29 of Glu, using 1-naphthyl acetyl spermine (NASPM), a selective open-channel blocker for  
30 GluA2-lacking calcium-permeable AMPARs<sup>70,71</sup>. Applying 1  $\mu$ M NASPM produced near-  
31 complete inhibition of the Glu-evoked current for WT GluA3 and most variants (Fig. 2C-D;

1 Supplementary Table S3). However, for two variants (p.(Arg631Ser) and p.(Ala654Pro)),  
2 NASPM application inhibited the membrane current below the level observed in the absence of  
3 Glu (Fig. 2C), indicating constitutive channel activity. This effect was most profound for the  
4 variant p.(Ala654Pro) (Fig. 2D; Supplementary Table S3). Specifically, in the absence of an  
5 agonist and at a holding potential of -40 mV, XOs expressing the p.(Ala654Pro) variant  
6 displayed approximately 10-fold increased membrane current ( $564 \pm 123$  nA;  $n = 21$ ) compared  
7 to XOs expressing the WT (receptor  $61 \pm 32$  nA;  $n = 20$ ). Also, the elevated membrane current  
8 for p.(Ala654Pro) increased relatively little upon Glu application in the presence of block of  
9 desensitization ( $I_{\text{GLU+CTZ}} = 89 \pm 20$  nA;  $n = 18$ ) compared to the membrane current in WT  
10 expressing ( $I_{\text{GLU+CTZ}} = 4230 \pm 490$  nA;  $n = 140$ ), but decreased by more than 300% upon  
11 NASPM application (Fig. 2D; Supplementary Table S3). Three variants (p.(Ala615Val),  
12 p.(Met617Thr), and p.(Gly826Asp) showed decreased inhibition by NASPM. These variants  
13 change residues located close to the NASPM binding site in the channel, and the decreased  
14 inhibition by NASPM likely reflects a direct effect on the binding affinity of NASPM<sup>72</sup>.

15 The TEVC functional characterizations of the 43 missense *GRIA3* variants showed that  
16 70% (30/43) changed one or more of the evaluated receptor parameters. As summarized in Fig.  
17 2E, 18 of the missense variants showed a pattern of functional effects that point to an overall LoF  
18 effect on receptor signalling function, including decreased or complete loss of desensitized and  
19 non-desensitized current response to Glu (no or decreased  $I_{\text{GLU}}$  or  $I_{\text{GLU+CTZ}}$ , respectively),  
20 reduced agonist sensitivity (increased  $EC_{50}$ ), reduced activation ability (decreased  $I_{\text{KA}}/I_{\text{GLU}}$  ratio),  
21 or increased desensitization (decreased  $I_{\text{GLU}}/I_{\text{GLU+CTZ}}$  ratio). In contrast, 12 variants showed effect  
22 patterns that suggest an overall GoF effect; *e.g.*, increased current amplitudes, agonist sensitivity,  
23 activation, including constitutive activity, and significantly reduced or completely blocked  
24 desensitization (Fig. 2F). Two variants (p.(Trp799Leu) and p.(Ser531Cys)) showed a mixed  
25 pattern of both GoF and LoF effects. Specifically, these variants showed no (p.(Ser531Cys)) or  
26 greatly reduced (p.(Trp799Leu)) desensitized current, but WT-like current amplitude upon block  
27 of desensitization (Fig. 1B-C, Supplementary Table S2 and S3). These results suggest a LoF  
28 functional phenotype due to increased desensitization. On the other hand, both variants decreased  
29 Glu  $EC_{50}$  dramatically (Fig. 1E; measured in the presence of CTZ), which is a GoF effect, and  
30 for p.(Trp799Leu) also increased the KA efficacy, indicating increased ability to be activated  
31 (Fig. 1B, Supplementary Table S3). However, we classified both variants to have an overall LoF

1 effect based on the reduced Glu current without blocked desensitization. Lastly, 13 variants did  
2 not show significant changes in any of the evaluated functional parameters (Fig. 2G) and,  
3 therefore, appeared neutral for the core ligand-gated channel function and were not investigated  
4 further. However, we cannot rule out that these variants may affect other aspects of GluA3-  
5 containing receptors beyond the functions studied here, such as receptor trafficking, regulation,  
6 and interactions with synaptic proteins important for native AMPARs.

7 The domain distribution of the GoF, LoF, and functionally neutral variants shows that  
8 GoF and LoF variants exclusively affect residues in the ABD, TMD, and ABD-TMD linkers,  
9 whereas most neutral variants affect residues in the NTD and CTD (Fig. 2E-G). Overall, the  
10 positions in the GluA3 sequence that are affected by LoF and GoF variants fit well with analysis  
11 of missense tolerance ratio<sup>73</sup> (MTR) (Fig. 2H), as 87% (27/31) of the variants with functional  
12 LoF or GoF affect residues in segments that appear highly intolerant to missense variation (Fig.  
13 2H), whereas 69% (9/13) of the functionally neutral variants affect positions with no unusual  
14 sensitivity to missense variation. This observation suggests that MTR analysis is a highly  
15 effective predictor of potential pathogenicity of missense variants for *GRIA3*. In comparison, the  
16 accuracy of the *in silico* prediction tools SIFT and PolyPhen in predicting the LoF/GoF variants  
17 as pathogenic was 72% and 74%, respectively (Supplementary Table S1).

18

## 19 ***GRIA3* variant effects are dominant in heteromeric AMPA** 20 **receptors**

21 GluA3 subunits are thought to preferentially assemble with GluA2 subunits into heteromeric  
22 GluA2/3 receptors in the brain, although triheteromeric GluA1/2/3 receptors have also recently  
23 been shown<sup>74-77</sup>. Thus, native GluA3-containing AMPARs in affected patients will have two  
24 subunits containing the variant. To assess whether variant effects were also present in  
25 heteromeric GluA2/A3 receptors, we expressed the LoF or GoF variants together with WT  
26 GluA2 and determined desensitized and non-desensitized current amplitudes, the degree of  
27 desensitization, and the KA/GLU response ratio (Fig. 3A-C; Supplementary Table S4). For each  
28 variant expressed with GluA2, the current-voltage (IV) relationship was determined, as this  
29 provides a measure for formation of heteromeric GluA2/A3 receptors (Fig. 3E). Specifically,

1 incorporation of GluA2 subunits shifts the IV curve from inwardly-rectifying to linear (as  
2 illustrated for WT and selected variants in Fig. 3E). All functional variants exhibited linear IV  
3 relationships when expressed with GluA2, which shows that the variants retain their ability of  
4 GluA3 to form heteromeric GluA2/A3 receptors. As summarized in Fig. 3D, the results showed  
5 that GoF effects observed in homomeric GluA3 were highly penetrant to heteromeric GluA2/A3.  
6 Specifically, significant changes for the affected parameters were also observed in GluA2/A3  
7 receptors for all variants exhibiting one or more GoF effects. Similarly, for variants that induced  
8 a LoF phenotype for homomeric GluA3, LoF effects were also observed in the heteromeric  
9 receptor background. Notably, among the variants that completely abolished the Glu response in  
10 homomeric GluA3 (p.(Gly492Ser), p.(Gly630Arg), p.(Met706Thr), p.(Gly721Arg),  
11 p.(Glu787Lys), p.(Glu787Gly), and p.(Gly833Arg)), currents could be measured for all when  
12 expressed as heteromers with GluA2, although with profoundly lower current amplitudes than  
13 WT GluA2/A3 (Fig. 3D, Supplementary Table S2). The only exception was the p.(Gly721Arg)  
14 variant, which showed a current amplitude similar to WT in heteromeric GluA2/A3 receptors  
15 (Supplementary Table S2). For all of these variants, a linear IV relationship similar to WT  
16 GluA2/3 was observed (Supplementary Fig. S3), confirming the presence of the GluA2 subunit  
17 in the heteromeric receptor complex.

18 In summary, the characterization of the effects of the 43 *GRIA3* missense variants  
19 revealed 31 (72%) to alter electrophysiological functions in both homomeric GluA3 and  
20 heteromeric GluA2/3 receptors, strongly indicating these variants as pathogenic.

21

## 22 **Kinetic characterization and classification of the pathogenic** 23 **variants**

24 Based on the TEVC evaluations, we next aimed to collect detailed phenotypic and genetic  
25 information from patients carrying the 31 *GRIA3* variants associated with significant LoF or GoF  
26 effects on receptor function and, therefore, are strongly indicated as a monogenetic cause of  
27 NDD. For 17 of these variants, we obtained detailed clinical information from 25 NDD patients,  
28 resulting in a cohort of 14 males (patients M1-M14) and 11 females (patients F1-F11). The  
29 genetic and phenotypic details of the patient cohort are described in the Supplementary results

1 and Supplementary Table S7. To further characterize how the 17 cohort variants perturb the  
2 receptor functional phenotype, we utilized fast-application patch-clamp electrophysiology, which  
3 can model the synaptic Glu pulses that evoke EPSCs on a millisecond timescale and can  
4 accurately identify changes in receptor deactivation and desensitization rates that are particularly  
5 important for shaping AMPAR synaptic signals. Specifically, the cohort variants were expressed  
6 in HEK293 cells as homomeric GluA3 and heteromeric GluA2/A3 receptors. Current responses  
7 to pulses of 10 mM Glu were recorded (*Materials & Methods*) (see Fig. 4A for an illustration of  
8 the recording protocol and representative current traces), except for variants p.(Ala653Thr),  
9 p.(Gly630Arg), and p.(Arg660Thr), which have previously been characterized with fast-  
10 application patch-clamp electrophysiology in both homomeric GluA3 and heteromeric  
11 GluA2/A3 receptors<sup>29,34,61</sup>. AMPAR subunits occur in two isoforms, denoted flip and flop, which  
12 result from alternative splicing of the two mutually exclusive exons, 14 and 15, respectively, and  
13 have important differences in receptor kinetics<sup>78</sup>. This alternative flip/flop splicing affects nine  
14 amino acid positions in a 38 amino acid segment close to the ABD-M4 linker. The  
15 p.(Glu787Gly) (patient M7), p.(Glu787Lys) (patient M8-9, F11), and p.(Trp799Leu) (patient F9)  
16 variants originate in exon 14 and specifically affect the flop isoform. Therefore, these variants  
17 were characterized in the flop isoform of GluA3 (GluA3<sub>o</sub>). The remaining variants are located  
18 outside the flip/flop segment and were characterized in the flip isoform (GluA3<sub>i</sub>), which  
19 predominates before birth and continues to be expressed in the adult brain<sup>79</sup>.

20 The results showed a complete or very severe LoF effect on the current response to fast  
21 Glu applications for the variants p.(Gly492Ser) (patient M2), p.(Phe655Ser) (patient M10),  
22 p.(Ile665Thr) (patient F10), and p.(Glu787Gly) (patient M7) (Fig. 4A). In addition, the variants  
23 p.(Gly630Arg) (patients M3-6) and p.(Glu787Lys) (patient M8-9, F11) that previously have been  
24 characterized with identical recording protocols, also have a complete LoF phenotype<sup>61</sup>.  
25 Moreover, expressed together with WT GluA2, all these variants also abolished the current  
26 response in heteromeric GluA2/A3 receptors, except for p.(Ile665Thr) (patient F10), which  
27 showed a robust and desensitizing current response (Fig. 4A). To test whether the complete or  
28 severe LoF effect was due to the variants perturbing expression and folding of the GluA3 subunit  
29 protein, or subunit ability to assemble into receptors that traffic to the membrane, we expressed  
30  $\beta$ -lac-tagged WT and variant GluA3 constructs in HEK293 cells (Supplementary methods).  
31 Analysis of the conversion rates of the  $\beta$ -lac substrate nitrocefin from transfected HEK293 cells

1 revealed no significant difference in cell-surface expression between WT and variant receptors  
2 (Supplementary Fig. S4). Thus, we conclude that the LoF effect that these variants have on Glu  
3 current is due to disruption of the core ligand-gated channel function of the receptor. The  
4 p.(Trp799Leu) variant showed measurable currents but with greatly reduced peak amplitude. In  
5 homomeric GluA3, due to the reduced currents we were only able to reliably determine the  
6 desensitization rate of the p.(Trp799Leu) variant in a single experiment, which showed 3-fold  
7 increased rate of desensitization ( $\tau_{\text{des}} = 0.57$  ms versus  $1.58 \pm 0.05$  ms;  $n = 15$  for WT GluA3<sub>o</sub>)  
8 and no measurable steady-state current (Fig. 4A-B; Supplementary table S5). These effects were  
9 also observed in the heteromeric GluA2/A3 receptor (Fig. 4A-B; Supplementary table S5), where  
10 slightly more robust currents allowed us to accurately determine the desensitization kinetics. and  
11 suggest p.(Trp799Leu) is a severe LoF variant by greatly reducing charge transfer due to an  
12 increased rate and extent of receptor desensitization. Notably, this is supported by the TEVC  
13 characterizations that showed that the diminished Glu current for p.(Trp799Leu) could be fully  
14 rescued by the pharmacological block of desensitization (Fig. 2 and 3).

15 The GoF variants p.(Ala654Val), p.(Ala654Thr), p.(Ala654Pro), p.(Ser663Pro),  
16 p.(Lys701Glu), p.(Gly803Ala), and p.(Gly803Glu) all produced robust currents when expressed  
17 as homomeric and heteromeric receptors (Fig. 4A). For these variants we determined the  
18 desensitization rate ( $\tau_{\text{des}}$ ) and peak-to-steady-state current ratio ( $I_{\text{ss}}$ ) from 500 ms glutamate  
19 stimulations (Fig. 4B-C) and the deactivation rate ( $\tau_{\text{deact}}$ ) from 1 ms stimulations (Fig. 4D-E,  
20 Supplementary table S5) (Materials and methods). As predicted from the TEVC results,  
21 p.(Ala654Val) (patient F5), p.(Ala654Thr) (patient F7), and p.(Ala654Pro) (patient F6) displayed  
22 greatly decreased desensitization. Specifically, whereas WT GluA3<sub>i</sub> currents almost completely  
23 decayed within milliseconds ( $\tau_{\text{des}} = 5.3 \pm 0.3$  ms;  $n = 12$ ) to a small fraction of the peak current  
24 ( $I_{\text{ss}} = 1.1 \pm 0.1\%$ ;  $n = 16$ ), the p.(Ala654Pro) variant completely blocked ( $I_{\text{ss}} = 100 \pm 0.0\%$ ,  $n =$   
25 4), and the p.(Ala654Thr) and p.(Ala654Val) variants greatly reduced the level of desensitization  
26 ( $I_{\text{ss}} = 82 \pm 3\%$ ,  $n = 9$ , and  $61 \pm 2\%$ ,  $n = 9$ , respectively). In addition, the deactivation rates for  
27 these variants were also slowed ( $\tau_{\text{deact}} = 5-22$  ms;  $n = 3-9$ ) compared to WT ( $\tau_{\text{deact}} = 2.1 \pm 0.2$   
28 ms;  $n = 9$ ) for homomeric GluA3 receptors (Fig. D-E, Supplementary table S5). These effects  
29 were maintained for the heteromeric GluA2/A3 receptor, where the p.(Ala654Pro) variant  
30 completely blocked desensitization and slowed deactivation, and the p.(Ala654Val) and  
31 p.(Ala654Thr) decreased desensitization and slowed deactivation, except for p.(Ala654Val),

1 which showed a deactivation rate not different from WT (Fig. B-C, Supplementary table S5).  
2 Thus, the three variants affecting Ala654 can be classified as severe GoF due to profoundly  
3 decreased desensitization and reduced deactivation rates. The variants p.(Ser663Pro) (patient F4)  
4 and p.(Lys701Glu) (patient F3) displayed phenotypes quite similar to each other, which included  
5 significantly increased  $I_{ss}$  levels, slowed desensitization rates, and modestly but significantly  
6 slowed deactivation rates in both homomeric and heteromeric receptors (Fig. B-C,  
7 Supplementary table S5). Lastly, the two variants affecting Gly803 (p.(Gly803Ala) and  
8 p.(Gly803Glu)) showed normal  $I_{ss}$  levels but reduced desensitization and deactivation rates (Fig.  
9 B-C, Supplementary Table S5). These changes, as a consequence of p.(Ser663Pro),  
10 p.(Lys701Glu), p.(Gly803Ala), and p.(Gly803Glu) variants, are predicted to have a clear GoF  
11 effect on the synaptic charge carried by GluA3-containing AMPARs, although to a less severe  
12 extent than the variants affecting Ala654.

13

## 14 **Correlation of LoF and GoF receptor effects with patient clinical** 15 **phenotype**

16 We next compared patient clinical information with the receptor phenotypic information. As  
17 summarized in Fig. 5A, we classified the variants based on the GoF and LoF effects identified in  
18 the electrophysiological analyses as severe or mild. In addition, data from previously reported  
19 evaluations of the p.(Ala653Thr)<sup>29</sup> and p.(Arg660Thr)<sup>34</sup> variants were included. For LoF  
20 variants, the severe class includes seven variants in 11 patients (M1-M10 and -F10; Fig. 5A) that  
21 completely abolish the current response to millisecond Glu stimulation, whereas the mild class  
22 includes two variants from three patients (p.(Ala653Thr) in patients M11-12 and p.(Trp799Leu)  
23 in patient F9), which show current response to fast Glu stimulation, but with greatly reduced  
24 amplitude and profound changes in desensitization and deactivation kinetics that overall are  
25 predicted to reduce synaptic charge transfer. For GoF variants, the mild class includes four  
26 patients with variants p.(Gly803Ala) (patient M13) and p.(Gly803Glu) (patients M14 and F1-2),  
27 which slow desensitization and deactivation rates significantly and increase Glu sensitivity, but  
28 do not appear to change peak or desensitized current levels. The severe GoF class includes the  
29 variants p.(Ala654Val), p.(Ala654Pro), and p.(Ala654Thr) (patients F5-F7, respectively)), in  
30 addition to p.(Ser663Pro) (patient F4)), p.(Arg660Thr) (patient F8)), and p.(Lys701Glu) (patient



1 F3), which all significantly reduce desensitization and deactivation rates, increase Glu sensitivity  
2 and increase steady-state current amplitudes in the TEVC experiments (Fig. 5A).

3 Several differences between the GoF and LoF patient classes (10 patients with GoF  
4 variants and 15 patients with LoF variants) were identified (Table 1 and Fig. 5B). Importantly,  
5 LoF and GoF variants are disease-causing in both sexes but affected males predominantly  
6 (12/14) carry hemizygous LoF variants. In contrast, most affected females (8/11) carry  
7 heterozygous GoF variants. Another striking difference includes the age of seizure onset in the  
8 subgroup of patients with epileptic comorbidities, muscle tone (hypo- versus hypertonia), sleep  
9 difficulties, and movement disorders, including hyperekplexia (Fig. 5B and Table 1).  
10 Specifically, for the patients with epileptic comorbidities, the median age of seizure onset in  
11 patients harboring a GoF was 1 month (range 1st day-12 months,  $n = 5$ ), being significantly  
12 earlier than in patients with LoF variants, being 16.5 months (range 12-36 months,  $n = 6$ ,  $P =$   
13  $0.004$ ). We detected no significant differences between the GoF and LoF groups when  
14 comparing seizure types ( $P = 0.85$ ) and treatment response ( $P = 1$ ). For body tone, most patients  
15 harboring a LoF variant had congenital muscular hypotonia ( $n = 10/15$ ), which was not reported  
16 in any of the 10 patients with GoF variants ( $P = 0.0004$ ). In contrast, congenital muscular  
17 hypertonia was present in 8/10 patients with GoF variants, while it was only reported in 1/15  
18 patients with LoF variants ( $p = 0.0002$ ). Sleep disturbances were reported in 10/15 patients with  
19 LoF variants, while they were only present in 2/10 patients with GoF variants ( $p = 0.0018$ ).  
20 Movement disorders of any kind were reported in 5/15 patients with LoF variants, while they  
21 were present in 8/10 patients with a GoF variant ( $p = 0.04$ ). In particular, an excessive startle  
22 response to external stimuli, also known as hyperekplexia, was more prevalent in the group with  
23 GoF variants ( $n = 5$ ) compared to the group with LoF variants ( $n = 1$ ) ( $p = 0.003$ ). For  
24 behavioural abnormalities, aggressive outbursts were more prevalent in the LoF cohort ( $n = 6$ )  
25 compared to the GoF cohort ( $n = 2$ ), although the difference was not significant ( $p = 0.29$ ). There  
26 were no significant differences in the other behavioural abnormalities reported in the GoF ( $n = 6$ )  
27 compared to the LoF cohort ( $n = 10$ ) ( $p = 0.75$ ). Although all patients had ID, we found no  
28 significant difference in severity between the GoF and LoF cohorts ( $p = 0.26$ ). Specifically, ID  
29 was reported to be borderline/mildly ( $n = 1$ ), moderately ( $n = 5$ ), severely ( $n = 8$ ), or profoundly  
30 ( $n = 1$ ) affected in the LoF cohort, while moderately ( $n = 4$ ), severely ( $n = 3$ ) or profoundly ( $n =$   
31  $3$ ) affected in the GoF cohort.

1 In summary, the phenotypic assessment indicates that GoF variants are objectively  
2 associated with more severe outcomes: patients were younger at the time of seizure onset,  
3 hypertonic, and more often had movement disorders, including hyperekplexia. In contrast,  
4 patients with LoF variants were older at seizure onset, hypotonic, and had sleep difficulties.  
5

## 6 Discussion

7 Missense variants in *GRIA3* are by far the most prevalently reported *GRIA* genetic defects in  
8 NDD patients. However, the extent to which the variants underlie NDDs is not clear, as few have  
9 been studied in cellular or animal models to confirm them as pathogenic variations. The present  
10 work systematically evaluates 44 rare *GRIA3* variants in NDD patients to establish whether these  
11 have functional effects on GluA3-containing AMPARs. Focusing on effects on core ligand-gated  
12 ion channel function, we find that 31 variants produced significant effects and were classified as  
13 LoF or GoF concerning overall receptor signalling capability. We correlate the identified effects  
14 on receptor function with the clinical features and find distinct GoF and LoF phenotypes. This  
15 specific LoF-GoF difference in clinical phenotype is in line with several other central nervous  
16 system (CNS) ion channel gene families, including the *GRIN* iGluR gene subfamily<sup>80</sup>, where  
17 studies applying detailed electrophysiological analysis of rare missense variant effects have  
18 established both LoF and GoF effects as pathogenic, with each category often leading to  
19 different disease phenotypes<sup>81–86</sup>. In addition to the clinical importance of providing a diagnosis  
20 and new disease understanding, identifying pathogenic variants as having LoF or GoF effects on  
21 channel function is also of therapeutic relevance as it potentially guides pharmacological  
22 intervention. For the iGluR gene families, this approach of systematic and detailed testing of  
23 pathogenic variants from patient cohorts and their clinical and therapeutic relevance has been  
24 successfully implemented for the NMDAR-encoding *GRIN* gene family, leading to a definition  
25 of specific neurological conditions associated with types of variant effect and examples of  
26 successful therapeutic intervention<sup>64,87,88</sup>. In this paper, we extend the value of this approach to  
27 the *GRIA* family. Moreover, our data advances the understanding of the role of abnormal  
28 function of AMPARs in general and GluA3-containing subtypes in particular in NDD  
29 syndromes. Firstly, as 71% of the evaluated variants altered GluA3-containing AMPAR  
30 function, *GRIA3* can be firmly classified as a general disease gene in NDDs, and underscores the

1 importance of appropriate AMPAR signalling for CNS development, as also suggested in single  
2 case or smaller cohort studies for *GRIA1*, *GRIA2*, and *GRIA3*<sup>22,29,30,32–34</sup>. Secondly, our work  
3 expands the spectrum and frequency of functional effects of pathogenic *GRIA3* variants by  
4 identifying distinct types of LoF and GoF effects and providing clear genotype-phenotype  
5 correlations that define two clinical phenotypes associated with predicted LoF and GoF effects:  
6 LoF variants often lead to muscular hypotonia, hyporeflexia, a sleep disorder, aggressive  
7 behaviour and later onset of seizures, whereas GoF variants are associated with muscular  
8 hypertonia, hyperreflexia, startle-induced non-epileptic myoclonia and earlier onset of seizures.

9         Although the GoF variants appear to be associated with more severe outcomes, such as  
10 earlier seizure onset and a higher prevalence of movement disorders, including hyperekplexia, all  
11 patients present with overall severe NDD phenotypes independent of the type of LoF or GoF  
12 effect of the *GRIA3* variants. This observation suggests that even quantitatively small alterations  
13 from WT AMPAR function lead to severe outcomes, which likely reflects the crucial role of  
14 AMPARs in the ability of excitatory synapses to detect transmission events rapidly. As  
15 excitatory synaptic currents can occur at rates of up to several hundred Hz, AMPARs have likely  
16 evolved with precisely balanced Glu sensitivity and extremely fast rates of activation,  
17 desensitization, and deactivation within a very narrow range. Thus, although some LoF and all  
18 GoF effects do not prevent the contribution of GluA3-containing AMPARs to synaptic  
19 transmission, they are likely to perturb the fidelity of neuronal activation. It is also noteworthy  
20 that patient M1, who is hemizygous for the protein-truncating complete LoF variant  
21 p.(Gln371Argfs\*6), appears to have the least severe symptoms compared to those with missense  
22 LoF variants, in particular in respect to the severity of ID (Table 1). This finding suggests that  
23 the complete loss of GluA3-containing receptors from synaptic AMPAR populations is better  
24 tolerated than the existence of GluA3-containing receptors with perturbed function. Interestingly,  
25 similar findings have been reported for  $\gamma$ -Aminobutyric acid A (GABA<sub>A</sub>) receptors<sup>89</sup>. Further  
26 detailed evaluation of more pathogenic *GRIA3* variants is warranted to explore how clinical  
27 severity correlates to variant effects on receptor function and will likely require establishing  
28 models for studying the variant impact on synaptic transmission and animal behavioural  
29 phenotypes.

30         The current data set also provides insight into emerging associations among sex and  
31 inheritance, which often is complicated for morbid genes on the X-chromosome, as it is not

1 always possible to predict the phenotypical effect in heterozygous females. Our data set  
2 establishes that LoF and GoF variants as disease-causing in both sexes, but that affected males  
3 more often (12/14) carry hemizygous LoF variants, whereas most affected females (8/11) carry  
4 heterozygous GoF variants. Although our data do not support a strict model, the prevalence of *de*  
5 *novo* GoF in females is consistent with the general understanding that LoF variants are likely to  
6 be less harmful in heterozygous females<sup>90</sup>. However, evaluation of further *GRIA3* variants in  
7 males and females is needed to explore *i*) the prevalence of GoF variants in females and LoF  
8 variants in males and *ii*) to describe if males with GoF variants are equally or more severely  
9 affected than females with similar variants.

10 Next-generation sequencing has become routine in hospitals, and the number of NDD  
11 patients with a genetic etiology is increasing<sup>91,92</sup>. As a result, the number of new *GRIA* variants  
12 needing a functional assessment is expected to rise. In addition to confirming pathogenicity,  
13 functional testing provides knowledge crucial for treatment, as choosing the right drug (effective  
14 and not exacerbating the existing symptoms) depends on establishing LoF or GoF status. In this  
15 respect, establishing the impact of new variants on AMPAR function via electrophysiological  
16 evaluation may become a critical bottleneck in individual cases, highlighting a need to develop  
17 approaches for the theoretical prediction of variant pathogenicity and LoF/GoF effects. Notably,  
18 recent large-scale bioinformatical efforts for exploring new approaches for prediction of  
19 pathogenicity of variants in genes encoding voltage- and ligand-gated ion channel subunits have  
20 suggested that clinical decision support algorithms that predict LoF/GoF status based on location  
21 in protein structure may become feasible<sup>93</sup>. Specifically, it was shown that certain positional  
22 measures of the variant in the structures of voltage-gated sodium channels and NMDA receptors  
23 could be correlated to functional effect and clinical phenotype<sup>93</sup>. For similar purpose in GluA3-  
24 containing AMPA receptors, we note that when considering the variant distribution throughout  
25 the GluA3 structure, it is observed that functionally neutral variants are enriched in the NTD,  
26 whereas LoF or GoF variants localize in the ABD, linker, and TMD segments (Fig. 1 and 2).  
27 However, we find several examples of close clustering of neutral, LoF, and GoF variants in these  
28 domains, which suggests that the clinical interpretation of missense variants in *GRIA3* as well as  
29 GoF/LoF classifications based on general localization measures in the receptor structure should  
30 be cautious.

1 For several pathogenic *GRIA3* variants, our analysis allows us to pinpoint the mechanistic  
2 cause of the overall LoF or GoF effect. This knowledge provides an opportunity for exploring  
3 clinically relevant AMPAR drugs for the pharmacological rescue of receptor function among  
4 different classes of variant phenotypes. Notably, for variants with LoF effects on AMPAR  
5 kinetics, positive allosteric modulators (PAMs) exist, in particular of the *ampakine* class, that can  
6 modulate AMPAR current amplitude and waveform via selective effects on receptor kinetics<sup>94</sup>.  
7 Although no AMPAR PAM currently is FDA/EMA approved, several have passed Phase I/II  
8 clinical trials, such as CX516<sup>95</sup>, CX717 (Fasoracetam)<sup>96</sup>, Org 24448 (Aniracetam)<sup>97</sup>, and  
9 CX1739<sup>98</sup>, including early proof-of-concept trials in patients with cognitive impairments<sup>99</sup>, and  
10 are subjects for ongoing clinical development. Similarly, for variants with GoF effects (e.g.,  
11 increased activation or decreased desensitization), negative allosteric modulators (NAMs) can be  
12 explored, including perampanel, which inhibits activation and accelerates desensitization<sup>100</sup>.  
13 Importantly, perampanel is approved for chronic treatment of several types of epilepsy<sup>101</sup>, and  
14 therefore, directly available as a potential precision medicine for patients with GoF AMPAR  
15 mutations, as recently has been demonstrated for GoF variants in other *GRIA* genes<sup>102</sup>.

16 The present study represents the largest functional evaluation of missense variants in any  
17 *GRIA* gene. Together with previous work on *GRIA1*, *GRIA2*, and *GRIA3*, the volume of  
18 validated pathogenic *GRIA* variants has now reached a critical point that firmly establishes *GRIA*  
19 genetic defects as the cause of an emerging neurological disease, recently referred to as *GRIA*  
20 disorder<sup>102</sup>. However, further understanding of *GRIA* disorder disease mechanisms and  
21 potentially devising standard rescue pharmacological strategies is complicated by the diversity of  
22 the native AMPAR subtypes that a pathogenic variant can affect. Notably, we focused our  
23 functional work on the homomeric GluA3 and the heteromeric GluA2/A3 subtypes in two  
24 heterologous expression models, which lack the postsynaptic proteins that interact with native  
25 AMPARs and contribute to their synaptic functions. Most native AMPARs assemble with  
26 different transmembrane AMPA receptor regulatory proteins (TARPs), which act as auxiliary  
27 subunits and have distinct effects on receptor function, including modulation of receptor gating  
28 and desensitization properties<sup>64,103</sup>. These effects may have significant implications for the  
29 variant effect on synaptic transmission, and further work is required to provide insights into how  
30 *GRIA* variants affect AMPAR function involving auxiliary subunits. Also, the absence of a  
31 neuronal environment presents a caveat to the classification of variants that do not display

1 functional effects, as functionally neutral variants may have detrimental effects on other aspects  
2 of AMPAR cellular biology, such as receptor incorporation and positioning at synapses and  
3 regulation during synaptic plasticity mechanisms. Specifically, our evaluation did not reveal  
4 effects on the core function of GluA3-containing AMPARs for 13 variants when evaluated in  
5 recombinant GluA3 receptors (Fig. 1). Recent progress in mapping the AMPAR interactome in  
6 the brain shows that native AMPARs during the receptor lifetime interact with more than 40  
7 intracellular, extracellular, or membrane-embedded proteins, which are important for proper  
8 receptor biogenesis, postsynaptic positioning, and function<sup>104</sup>. We cannot rule out that apparently  
9 neutral variants may indeed influence expression and function of native GluA3-containing  
10 AMPARs by interfering with the ability of the GluA3 subunit to interact with synaptic  
11 constituents, and confident classification of *GRIA3* variants as neutral is thus not possible in  
12 current practise. Therefore, studies beyond establishing the functional defects of *GRIA* variants  
13 are needed to describe effects in a synaptic context. Importantly, the impact of LoF/GoF variants  
14 on the AMPAR-component of EPSC currents should be determined and correlated with the  
15 effects on kinetic parameters obtained from heterologous expression systems. This will improve  
16 the framework of predicting synaptic effects for variants based on functional evaluations in  
17 reduced systems such as XOs or HEK293 cells.

18 We have characterized the consequences of 44 *GRIA3* variants identified in NDD patients  
19 on GluA3-containing receptor function. Although the spectrum of variant effects on AMPAR  
20 signalling mechanisms that underlie the phenotype of each patient is likely to be complex, our  
21 analysis shows two significant genotype-phenotype correlations that correspond to predicted  
22 GoF or LoF effects on the signalling function of GluA3-containing AMPARs.

23

## 24 **Data availability**

25 The authors confirm that the data supporting the findings of this study are available in the main  
26 text and its supplementary material.

27

28

## 1 **Acknowledgements**

2 We thank the families for participating in this study. This study makes use of data generated by  
3 the DECIPHER community. A full list of centers that contributed to the generation of the data is  
4 available from <https://deciphergenomics.org/about/stats> and via e-mail from  
5 [contact@deciphergenomics.org](mailto:contact@deciphergenomics.org). Funding for the DECIPHER project was provided by Wellcome  
6 [grant number WT223718/Z/21/Z]. This work has been generated within the European Reference  
7 Network on Rare Congenital Malformations and Rare Intellectual Disability (ERN-ITHACA)  
8 [EU Framework Partnership Agreement ID: 3HP-HP-FPA ERN-01-2016/739516]. In addition,  
9 we thank the ERN EPICARE network for promoting our collaborative call on *GRIA*-related  
10 disorders.

11

## 12 **Funding**

13 AB (Allan Bayat) is funded by Novo Nordisk Foundation BRIDGE Programme  
14 (NNF20SA0064340). JHS (Jia-Hui Sun) is supported by the National Natural Science  
15 Foundation of China (32200779). The research conducted at the Murdoch Children's Research  
16 Institute (MCRI) was supported by the Victorian Government's Operational Infrastructure  
17 Support Program. The Royal Children's Hospital Foundation generously supports the Chair in  
18 Genomic Medicine awarded to JC. LCB (Lindsay Catherine Burrage) is supported by NIH  
19 (5U54OD030165). YSS (Yun Stone Shi) is supported by the National Key R & D Program of  
20 China (2019YFA0801603), the National Natural Science Foundation of China (32170951), the  
21 Fundamental Research Funds for the Central Universities (021414380533) and Special Fund for  
22 Science and Technology Innovation Strategy of Guangdong Province (2021B0909050004). ASK  
23 (Anders Skov Kristensen) is supported by Independent Research Fund Denmark (3101-00386B).

24

## 25 **Competing interests**

26 The authors report no competing interests.

27

# 1 **Supplementary material**

2 Supplementary material is available at *Brain* online.

3

## 4 **References**

- 5 1. Hansen KB, Wollmuth LP, Bowie D, et al. Structure, Function, and Pharmacology of  
6 Glutamate Receptor Ion Channels. *Pharmacol Rev.* 2021;73(4):298-487.  
7 doi:10.1124/pharmrev.120.000131
- 8 2. Raman IM, Trussell LO. The kinetics of the response to glutamate and kainate in neurons of  
9 the avian cochlear nucleus. *Neuron.* 1992;9(1):173-186. doi:10.1016/0896-6273(92)90232-3
- 10 3. Sah P, Hestrin S, Nicoll RA. Properties of excitatory postsynaptic currents recorded in vitro  
11 from rat hippocampal interneurons. *J Physiol.* 1990;430:605-616.  
12 doi:10.1113/jphysiol.1990.sp018310
- 13 4. Silver RA, Traynelis SF, Cull-Candy SG. Rapid-time-course miniature and evoked  
14 excitatory currents at cerebellar synapses in situ. *Nature.* 1992;355(6356):163-166.  
15 doi:10.1038/355163a0
- 16 5. Hayashi Y, Shi SH, Esteban JA, Piccini A, Poncer JC, Malinow R. Driving AMPA  
17 Receptors into Synapses by LTP and CaMKII: Requirement for GluR1 and PDZ Domain  
18 Interaction. *Science.* 2000;287(5461):2262 LP - 2267. doi:10.1126/science.287.5461.2262
- 19 6. Barria A, Muller D, Derkach V, Griffith LC, Soderling TR. Regulatory phosphorylation of  
20 AMPA-type glutamate receptors by CaM-KII during long-term potentiation. *Science.*  
21 1997;276(5321):2042-2045. doi:10.1126/science.276.5321.2042
- 22 7. Kauer JA, Malenka RC, Nicoll RA. A persistent postsynaptic modification mediates long-  
23 term potentiation in the hippocampus. *Neuron.* 1988;1(10):911-917. doi:10.1016/0896-  
24 6273(88)90148-1
- 25 8. Mahanty NK, Sah P. Calcium-permeable AMPA receptors mediate long-term potentiation in  
26 interneurons in the amygdala. *Nature.* 1998;394(6694):683-687. doi:10.1038/29312



- 1 9. Rumpel S, LeDoux J, Zador A, Malinow R. Postsynaptic Receptor Trafficking Underlying a  
2 Form of Associative Learning. *Science*. 2005;308(5718):83-88.  
3 doi:10.1126/science.1103944
- 4 10. Lee HK, Takamiya K, Han JS, et al. Phosphorylation of the AMPA Receptor GluR1 Subunit  
5 Is Required for Synaptic Plasticity and Retention of Spatial Memory. *Cell*. 2003;112(5):631-  
6 643. doi:10.1016/S0092-8674(03)00122-3
- 7 11. Esteban JA, Shi SH, Wilson C, Nuriya M, Huganir RL, Malinow R. PKA phosphorylation of  
8 AMPA receptor subunits controls synaptic trafficking underlying plasticity. *Nat Neurosci*.  
9 2003;6(2):136-143. doi:10.1038/nn997
- 10 12. Hu H, Real E, Takamiya K, et al. Emotion Enhances Learning via Norepinephrine  
11 Regulation of AMPA-Receptor Trafficking. *Cell*. 2007;131(1):160-173.  
12 doi:10.1016/j.cell.2007.09.017
- 13 13. Kessels HW, Malinow R. Synaptic AMPA Receptor Plasticity and Behavior. *Neuron*.  
14 2009;61(3):340-350. doi:10.1016/j.neuron.2009.01.015
- 15 14. Schwenk J, Baehrens D, Haupt A, et al. Regional diversity and developmental dynamics of  
16 the AMPA-receptor proteome in the mammalian brain. *Neuron*. 2014;84(1):41-54.  
17 doi:10.1016/j.neuron.2014.08.044
- 18 15. Swanson GT, Kamboj SK, Cull-Candy SG. Single-Channel Properties of Recombinant  
19 AMPA Receptors Depend on RNA Editing, Splice Variation, and Subunit Composition. *J*  
20 *Neurosci*. 1997;17(1):58-69. doi:10.1523/JNEUROSCI.17-01-00058.1997
- 21 16. Keinänen K, Wisden W, Sommer B, et al. A family of AMPA-selective glutamate receptors.  
22 *Science*. 1990;249(4968):556-560. doi:10.1126/science.2166337
- 23 17. Puckett C, Gomez CM, Korenberg JR, et al. Molecular cloning and chromosomal  
24 localization of one of the human glutamate receptor genes. *Proc Natl Acad Sci U S A*.  
25 1991;88(17):7557-7561. doi:10.1073/pnas.88.17.7557
- 26 18. Sun W, Ferrer-Montiel AV, Schinder AF, McPherson JP, Evans GA, Montal M. Molecular  
27 cloning, chromosomal mapping, and functional expression of human brain glutamate  
28 receptors. *Proc Natl Acad Sci U S A*. 1992;89(4):1443-1447. doi:10.1073/pnas.89.4.1443

- 1 19. Gécz J, Barnett S, Liu J, et al. Characterization of the human glutamate receptor subunit 3  
2 gene (GRIA3), a candidate for bipolar disorder and nonspecific X-linked mental retardation.  
3 *Genomics*. 1999;62(3):356-368. doi:10.1006/geno.1999.6032
- 4 20. Boulter J, Hollmann M, O'Shea-Greenfield A, et al. Molecular cloning and functional  
5 expression of glutamate receptor subunit genes. *Science*. 1990;249(4972):1033-1037.  
6 doi:10.1126/science.2168579
- 7 21. Hollmann M, O'Shea-Greenfield A, Rogers SW, Heinemann S. Cloning by functional  
8 expression of a member of the glutamate receptor family. *Nature*. 1989;342(6250):643-648.  
9 doi:10.1038/342643a0
- 10 22. Piard J, Béreau M, XiangWei W, et al. The GRIA3 c.2477G > A Variant Causes an  
11 Exaggerated Startle Reflex, Chorea, and Multifocal Myoclonus. *Mov Disord*.  
12 2020;35(7):1224-1232. doi:10.1002/mds.28058
- 13 23. Geisheker MR, Heymann G, Wang T, et al. Hotspots of missense mutation identify  
14 neurodevelopmental disorder genes and functional domains. *Nat Neurosci*. 2017;20(8):1043-  
15 1051. doi:10.1038/nn.4589
- 16 24. Hackmann K, Matko S, Gerlach EM, et al. Partial deletion of GLRB and GRIA2 in a patient  
17 with intellectual disability. *Eur J Hum Genet*. 2013;21(1):112-114. doi:10.1038/ejhg.2012.97
- 18 25. Salpietro V, Dixon CL, Guo H, et al. AMPA receptor GluA2 subunit defects are a cause of  
19 neurodevelopmental disorders. *Nat Commun*. 2019;10(1):3094. doi:10.1038/s41467-019-  
20 10910-w
- 21 26. Trivisano M, Santarone ME, Micalizzi A, et al. GRIA3 missense mutation is cause of an x-  
22 linked developmental and epileptic encephalopathy. *Seizure*. 2020;82:1-6.  
23 doi:10.1016/j.seizure.2020.08.032
- 24 27. Philips AK, Sirén A, Avela K, et al. X-exome sequencing in Finnish families with  
25 Intellectual Disability - Four novel mutations and two novel syndromic phenotypes.  
26 *Orphanet J Rare Dis*. 2014;9(1):49. doi:10.1186/1750-1172-9-49
- 27 28. Martin S, Chamberlin A, Shinde DN, et al. De Novo Variants in GRIA4 Lead to Intellectual  
28 Disability with or without Seizures and Gait Abnormalities. *Am J Hum Genet*.  
29 2017;101(6):1013-1020. doi:10.1016/j.ajhg.2017.11.004

- 1 29. Davies B, Brown LA, Cais O, et al. A point mutation in the ion conduction pore of AMPA  
2 receptor GRIA3 causes dramatically perturbed sleep patterns as well as intellectual  
3 disability. *Hum Mol Genet.* 2017;26(20):3869-3882. doi:10.1093/hmg/ddx270
- 4 30. Wu Y, Arai AC, Rumbaugh G, et al. Mutations in ionotropic AMPA receptor 3 alter channel  
5 properties and are associated with moderate cognitive impairment in humans. *Proc Natl  
6 Acad Sci U S A.* 2007;104(46):18163-18168. doi:10.1073/pnas.0708699104
- 7 31. Chérot E, Keren B, Dubourg C, et al. Using medical exome sequencing to identify the causes  
8 of neurodevelopmental disorders: Experience of 2 clinical units and 216 patients. *Clin Genet.*  
9 2018;93(3):567-576. doi:10.1111/cge.13102
- 10 32. Hamanaka K, Miyoshi K, Sun JH, et al. Amelioration of a neurodevelopmental disorder by  
11 carbamazepine in a case having a gain-of-function GRIA3 variant. *Hum Genet.* Published  
12 online January 15, 2022. doi:10.1007/s00439-021-02416-7
- 13 33. Rinaldi B, Ge YH, Freri E, et al. Myoclonic status epilepticus and cerebellar hypoplasia  
14 associated with a novel variant in the GRIA3 gene. *neurogenetics.* Published online  
15 November 3, 2021. doi:10.1007/s10048-021-00666-1
- 16 34. Sun JH, Chen J, Ayala Valenzuela FE, et al. X-linked neonatal-onset epileptic  
17 encephalopathy associated with a gain-of-function variant p.R660T in GRIA3. zhang wei,  
18 ed. *PLOS Genet.* 2021;17(6):e1009608. doi:10.1371/journal.pgen.1009608
- 19 35. Martinez-Estevé Melnikova A, Pijuan J, Aparicio J, et al. The p.Glu787Lys variant in the  
20 GRIA3 gene causes developmental and epileptic encephalopathy mimicking structural  
21 epilepsy in a female patient. *Eur J Med Genet.* 2022;65(3):104442.  
22 doi:10.1016/j.ejmg.2022.104442
- 23 36. Philippe A, Malan V, Jacquemont ML, et al. Xq25 duplications encompassing GRIA 3 and  
24 STAG 2 genes in two families convey recognizable X-linked intellectual disability with  
25 distinctive facial appearance. *Am J Med Genet A.* 2013;161(6):1370-1375.  
26 doi:10.1002/ajmg.a.35307
- 27 37. Chiyonobu T, Hayashi S, Kobayashi K, et al. Partial tandem duplication of GRIA3 in a male  
28 with mental retardation. *Am J Med Genet A.* 2007;143(13):1448-1455.  
29 doi:10.1002/ajmg.a.31798

- 1 38. Allen NM, Conroy J, Shahwan A, et al. Unexplained early onset epileptic encephalopathy:  
2 Exome screening and phenotype expansion. *Epilepsia*. 2016;57(1):e12-e17.  
3 doi:10.1111/epi.13250
- 4 39. Jacquemont ML, Sanlaville D, Redon R, et al. Array-based comparative genomic  
5 hybridisation identifies high frequency of cryptic chromosomal rearrangements in patients  
6 with syndromic autism spectrum disorders. *J Med Genet*. 2006;43(11):843-849.  
7 doi:10.1136/jmg.2006.043166
- 8 40. Guilmatre A, Dubourg C, Mosca AL, et al. Recurrent rearrangements in synaptic and  
9 neurodevelopmental genes and shared biologic pathways in schizophrenia, autism, and  
10 mental retardation. *Arch Gen Psychiatry*. 2009;66(9):947-956.  
11 doi:10.1001/archgenpsychiatry.2009.80
- 12 41. Bonnet C, Leheup B, Béri M, Philippe C, Grégoire MJ, Jonveaux P. Aberrant GRIA3  
13 transcripts with multi-exon duplications in a family with X-linked mental retardation. *Am J*  
14 *Med Genet A*. 2009;149(6):1280-1289. doi:10.1002/ajmg.a.32858
- 15 42. Yang Y, Muzny DM, Xia F, et al. Molecular findings among patients referred for clinical  
16 whole-exome sequencing. *JAMA*. 2014;312(18):1870-1879. doi:10.1001/jama.2014.14601
- 17 43. Hu H, Haas SA, Chelly J, et al. X-exome sequencing of 405 unresolved families identifies  
18 seven novel intellectual disability genes. *Mol Psychiatry*. 2016;21(1):133-148.  
19 doi:10.1038/mp.2014.193
- 20 44. LaDuca H, Farwell KD, Vuong H, et al. Exome sequencing covers >98% of mutations  
21 identified on targeted next generation sequencing panels. *PloS One*. 2017;12(2):e0170843.  
22 doi:10.1371/journal.pone.0170843
- 23 45. Hesse AN, Bevilacqua J, Shankar K, Reddi HV. Retrospective genotype-phenotype analysis  
24 in a 305 patient cohort referred for testing of a targeted epilepsy panel. *Epilepsy Res*.  
25 2018;144:53-61. doi:10.1016/j.eplepsyres.2018.05.004
- 26 46. Lyu Y, Yang Y, Liu Y, Gai Z. Analysis of a patient with X-linked mental retardation by next  
27 generation sequencing. *Zhonghua Yi Xue Yi Chuan Xue Za Zhi Zhonghua Yixue Yichuanxue*  
28 *Zazhi Chin J Med Genet*. 2018;35(2):257-260. doi:10.3760/cma.j.issn.1003-  
29 9406.2018.02.025

- 1 47. Bai Z, Kong X. X-linked mental retardation combined with autism caused by a novel  
2 hemizygous mutation of GRIA3 gene. *Zhonghua Yi Xue Yi Chuan Xue Za Zhi Zhonghua*  
3 *Yixue Yichuanxue Zazhi Chin J Med Genet.* 2019;36(8):829-833.  
4 doi:10.3760/cma.j.issn.1003-9406.2019.08.019
- 5 48. Carraro M, Monzon AM, Chiricosta L, et al. Assessment of patient clinical descriptions and  
6 pathogenic variants from gene panel sequences in the CAGI-5 intellectual disability  
7 challenge. *Hum Mutat.* 2019;40(9):1330-1345. doi:10.1002/humu.23823
- 8 49. Fernández-Marmiesse A, Roca I, Díaz-Flores F, et al. Rare Variants in 48 Genes Account for  
9 42% of Cases of Epilepsy With or Without Neurodevelopmental Delay in 246 Pediatric  
10 Patients. *Front Neurosci.* 2019;13. Accessed March 6, 2022.  
11 <https://www.frontiersin.org/article/10.3389/fnins.2019.01135>
- 12 50. Poot M, Eleveld MJ, van 't Slot R, Ploos van Amstel HK, Hochstenbach R. Recurrent copy  
13 number changes in mentally retarded children harbour genes involved in cellular localization  
14 and the glutamate receptor complex. *Eur J Hum Genet EJHG.* 2010;18(1):39-46.  
15 doi:10.1038/ejhg.2009.120
- 16 51. Alkelai A, Shohat S, Greenbaum L, et al. Expansion of the GRIA2 phenotypic  
17 representation: a novel de novo loss of function mutation in a case with childhood onset  
18 schizophrenia. *J Hum Genet.* 2021;66(3):339-343. doi:10.1038/s10038-020-00846-1
- 19 52. Latsko MS, Koboldt DC, Franklin SJ, et al. De novo missense mutation in GRIA2 in a  
20 patient with global developmental delay, autism spectrum disorder, and epileptic  
21 encephalopathy. *Cold Spring Harb Mol Case Stud.* 2022;8(4):a006172, mcs.a006172.  
22 doi:10.1101/mcs.a006172
- 23 53. Vijayaraghavan A, Urulangodi M, Ajit Valaparambil K, Sundaram S, Krishnan S. Movement  
24 Disorders in GRIA2-Related Disorder - Expanding the Genetic Spectrum of Developmental  
25 Dyskinetic Encephalopathy. *Mov Disord Clin Pract.* 2023;10(8):1222-1224.  
26 doi:10.1002/mdc3.13797
- 27 54. Cai Q, Zhou Z, Luo R, et al. Novel GRIA2 variant in a patient with atypical autism spectrum  
28 disorder and psychiatric symptoms: a case report. *BMC Pediatr.* 2022;22(1):629.  
29 doi:10.1186/s12887-022-03702-7

- 1 55. Okano S, Makita Y, Miyamoto A, et al. GRIA3 p.Met661Thr variant in a female with  
2 developmental epileptic encephalopathy. *Hum Genome Var.* 2023;10(1):1-4.  
3 doi:10.1038/s41439-023-00232-1
- 4 56. Wang H, Liu J, Li F, Teng Z, Liu M, Gu W. Novel Heterozygous Missense Variant in  
5 GRIA4 Gene Associated With Neurodevelopmental Disorder With or Without Seizures and  
6 Gait Abnormalities. *Front Genet.* 2022;13:859140. doi:10.3389/fgene.2022.859140
- 7 57. Ismail V, Zachariassen LG, Godwin A, et al. Identification and functional evaluation of  
8 GRIA1 missense and truncation variants in individuals with ID: An emerging  
9 neurodevelopmental syndrome. *Am J Hum Genet.* 2022;109(7):1217-1241.  
10 doi:10.1016/j.ajhg.2022.05.009
- 11 58. Firth HV, Richards SM, Bevan AP, et al. DECIPHER: Database of Chromosomal Imbalance  
12 and Phenotype in Humans Using Ensembl Resources. *Am J Hum Genet.* 2009;84(4):524-  
13 533. doi:10.1016/j.ajhg.2009.03.010
- 14 59. Landrum MJ, Lee JM, Benson M, et al. ClinVar: improving access to variant interpretations  
15 and supporting evidence. *Nucleic Acids Res.* 2018;46(D1):D1062-D1067.  
16 doi:10.1093/nar/gkx1153
- 17 60. Sobreira N, Schiettecatte F, Valle D, Hamosh A. GeneMatcher: a matching tool for  
18 connecting investigators with an interest in the same gene. *Hum Mutat.* 2015;36(10):928-  
19 930. doi:10.1002/humu.22844
- 20 61. Peng SX, Pei J, Rinaldi B, et al. Dysfunction of AMPA receptor GluA3 is associated with  
21 aggressive behavior in human. *Mol Psychiatry.* 2022;27(10):4092-4102.  
22 doi:10.1038/s41380-022-01659-8
- 23 62. Kiskin NI, Krishtal OA, Tsyndrenko AYa null. Excitatory amino acid receptors in  
24 hippocampal neurons: kainate fails to desensitize them. *Neurosci Lett.* 1986;63(3):225-230.  
25 doi:10.1016/0304-3940(86)90360-5
- 26 63. Otis T, Zhang S, Trussell LO. Direct measurement of AMPA receptor desensitization  
27 induced by glutamatergic synaptic transmission. *J Neurosci Off J Soc Neurosci.*  
28 1996;16(23):7496-7504. doi:10.1523/JNEUROSCI.16-23-07496.1996

- 1 64. Hansen KB, Wollmuth LP, Bowie D, et al. Structure, Function, and Pharmacology of  
2 Glutamate Receptor Ion Channels. *Pharmacol Rev.* 2021;73(4):298-487.  
3 doi:10.1124/pharmrev.120.000131
- 4 65. Stern-Bach Y, Russo S, Neuman M, Rosenmund C. A point mutation in the glutamate  
5 binding site blocks desensitization of AMPA receptors. *Neuron.* 1998;21(4):907-918.  
6 doi:10.1016/s0896-6273(00)80605-4
- 7 66. Suzuki E, Kessler M, Arai AC. The fast kinetics of AMPA GluR3 receptors is selectively  
8 modulated by the TARPs gamma 4 and gamma 8. *Mol Cell Neurosci.* 2008;38(1):117-123.  
9 doi:10.1016/j.mcn.2008.01.018
- 10 67. Pei W, Huang Z, Niu L. GluR3 flip and flop: Differences in channel opening kinetics.  
11 *Biochemistry.* 2007;46(7):2027-2036. doi:10.1021/bi062213s
- 12 68. Magazanik LG, Buldakova SL, Samoilova MV, Gmiro VE, Mellor IR, Usherwood PNR.  
13 Block of open channels of recombinant AMPA receptors and native AMPA/kainate  
14 receptors by Adamantane derivatives. *J Physiol.* 1997;505(3):655-663. doi:10.1111/j.1469-  
15 7793.1997.655ba.x
- 16 69. Hampson DR, Manalo JL. The activation of glutamate receptors by kainic acid and domoic  
17 acid. *Nat Toxins.* 1998;6(3-4):153-158. doi:10.1002/(sici)1522-  
18 7189(199805/08)6:3/4<153::aid-nt16>3.0.co;2-1
- 19 70. Tsubokawa H, Oguro K, Masuzawa T, Nakaima T, Kawai N. Effects of a spider toxin and its  
20 analogue on glutamate-activated currents in the hippocampal CA1 neuron after ischemia. *J*  
21 *Neurophysiol.* 1995;74(1):218-225. doi:10.1152/jn.1995.74.1.218
- 22 71. Koike M, Iino M, Ozawa S. Blocking effect of 1-naphthyl acetyl spermine on Ca(2+)-  
23 permeable AMPA receptors in cultured rat hippocampal neurons. *Neurosci Res.*  
24 1997;29(1):27-36. doi:10.1016/s0168-0102(97)00067-9
- 25 72. Twomey EC, Yelshanskaya MV, Vassilevski AA, Sobolevsky AI. Mechanisms of Channel  
26 Block in Calcium-Permeable AMPA Receptors. *Neuron.* 2018;99(5):956-968.e4.  
27 doi:10.1016/j.neuron.2018.07.027

- 1 73. Traynelis J, Silk M, Wang Q, et al. Optimizing genomic medicine in epilepsy through a  
2 gene-customized approach to missense variant interpretation. *Genome Res.*  
3 2017;27(10):1715-1729. doi:10.1101/gr.226589.117
- 4 74. Zhao Y, Chen S, Swensen AC, Qian WJ, Gouaux E. Architecture and subunit arrangement  
5 of native AMPA receptors elucidated by cryo-EM. *Science.* 2019;364(6438):355-362.  
6 doi:10.1126/science.aaw8250
- 7 75. Schwenk J, Harmel N, Brechet A, et al. High-resolution proteomics unravel architecture and  
8 molecular diversity of native AMPA receptor complexes. *Neuron.* 2012;74(4):621-633.  
9 doi:10.1016/j.neuron.2012.03.034
- 10 76. van der Spek SJF, Pandya NJ, Koopmans F, et al. Expression and Interaction Proteomics of  
11 GluA1- and GluA3-Subunit-Containing AMPARs Reveal Distinct Protein Composition.  
12 *Cells.* 2022;11(22):3648. doi:10.3390/cells11223648
- 13 77. Wenthold RJ, Petralia RS, Blahos J, Niedzielski AS. Evidence for multiple AMPA receptor  
14 complexes in hippocampal CA1/CA2 neurons. *J Neurosci.* 1996;16(6):1982-1989.  
15 doi:10.1523/jneurosci.16-06-01982.1996
- 16 78. Sommer B, Keinänen K, Verdoorn TA, et al. Flip and flop: A cell-specific functional switch  
17 in glutamate-operated channels of the CNS. *Science.* 1990;249(4976):1580-1585.  
18 doi:10.1126/science.1699275
- 19 79. Monyer H, Seeburg PH, Wisden W. Glutamate-operated channels: developmentally early  
20 and mature forms arise by alternative splicing. *Neuron.* 1991;6(5):799-810.  
21 doi:10.1016/0896-6273(91)90176-z
- 22 80. Strehlow V, Heyne HO, Vlaskamp DRM, et al. GRIN2A-related disorders: genotype and  
23 functional consequence predict phenotype. *Brain J Neurol.* 2019;142(1):80-92.  
24 doi:10.1093/brain/awy304
- 25 81. Wolff M, Johannesen KM, Hedrich UBS, et al. Genetic and phenotypic heterogeneity  
26 suggest therapeutic implications in SCN2A-related disorders. *Brain J Neurol.*  
27 2017;140(5):1316-1336. doi:10.1093/brain/awx054



- 1 82. Brunklaus A, Du J, Steckler F, et al. Biological concepts in human sodium channel epilepsies  
2 and their relevance in clinical practice. *Epilepsia*. 2020;61(3):387-399.  
3 doi:10.1111/epi.16438
- 4 83. Brunklaus A, Schorge S, Smith AD, et al. SCN1A variants from bench to bedside-improved  
5 clinical prediction from functional characterization. *Hum Mutat*. 2020;41(2):363-374.  
6 doi:10.1002/humu.23943
- 7 84. Masnada S, Hedrich UBS, Gardella E, et al. Clinical spectrum and genotype-phenotype  
8 associations of KCNA2-related encephalopathies. *Brain J Neurol*. 2017;140(9):2337-2354.  
9 doi:10.1093/brain/awx184
- 10 85. Johannesen KM, Liu Y, Koko M, et al. Genotype-phenotype correlations in SCN8A-related  
11 disorders reveal prognostic and therapeutic implications. *Brain J Neurol*. 2022;145(9):2991-  
12 3009. doi:10.1093/brain/awab321
- 13 86. Malerba F, Alberini G, Balagura G, et al. Genotype-phenotype correlations in patients with  
14 de novo KCNQ2 pathogenic variants. *Neurol Genet*. 2020;6(6):e528.  
15 doi:10.1212/NXG.0000000000000528
- 16 87. Benke TA, Park K, Krey I, et al. Clinical and therapeutic significance of genetic variation in  
17 the GRIN gene family encoding NMDARs. *Neuropharmacology*. 2021;199:108805.  
18 doi:10.1016/j.neuropharm.2021.108805
- 19 88. Han W, Yuan H, Allen JP, et al. Opportunities for Precision Treatment of GRIN2A and  
20 GRIN2B Gain-of-Function Variants in Triheteromeric N-Methyl-D-Aspartate Receptors. *J*  
21 *Pharmacol Exp Ther*. 2022;381(1):54-66. doi:10.1124/jpet.121.001000
- 22 89. Absalom NL, Liao VWY, Johannesen KMH, et al. Gain-of-function and loss-of-function  
23 GABRB3 variants lead to distinct clinical phenotypes in patients with developmental and  
24 epileptic encephalopathies. *Nat Commun*. 2022;13:1822. doi:10.1038/s41467-022-29280-x
- 25 90. Migeon BR. X-linked diseases: susceptible females. *Genet Med Off J Am Coll Med Genet*.  
26 2020;22(7):1156-1174. doi:10.1038/s41436-020-0779-4
- 27 91. Srivastava S, Love-Nichols JA, Dies KA, et al. Meta-analysis and multidisciplinary  
28 consensus statement: exome sequencing is a first-tier clinical diagnostic test for individuals

- 1 with neurodevelopmental disorders. *Genet Med.* 2019;21(11):2413-2421.  
2 doi:10.1038/s41436-019-0554-6
- 3 92. Krey I, Platzer K, Esterhuizen A, et al. Current practice in diagnostic genetic testing of the  
4 epilepsies. *Epileptic Disord Int Epilepsy J Videotape.* 2022;24(5):765-786.  
5 doi:10.1684/epd.2022.1448
- 6 93. Brünger T, Pérez-Palma E, Montanucci L, et al. Conserved patterns across ion channels  
7 correlate with variant pathogenicity and clinical phenotypes. *Brain J Neurol.*  
8 2023;146(3):923-934. doi:10.1093/brain/awac305
- 9 94. Arai AC, Kessler M. Pharmacology of ampakine modulators: from AMPA receptors to  
10 synapses and behavior. *Curr Drug Targets.* 2007;8(5):583-602.  
11 doi:10.2174/138945007780618490
- 12 95. Goff DC, Lamberti JS, Leon AC, et al. A placebo-controlled add-on trial of the Ampakine,  
13 CX516, for cognitive deficits in schizophrenia. *Neuropsychopharmacol Off Publ Am Coll*  
14 *Neuropsychopharmacol.* 2008;33(3):465-472. doi:10.1038/sj.npp.1301444
- 15 96. Wesensten NJ, Reichardt RM, Balkin TJ. Ampakine (CX717) effects on performance and  
16 alertness during simulated night shift work. *Aviat Space Environ Med.* 2007;78(10):937-943.  
17 doi:10.3357/asem.2055.2007
- 18 97. Senin U, Abate G, Fieschi C, et al. Aniracetam (Ro 13-5057) in the treatment of senile  
19 dementia of Alzheimer type (SDAT): results of a placebo controlled multicentre clinical  
20 study. *Eur Neuropsychopharmacol J Eur Coll Neuropsychopharmacol.* 1991;1(4):511-517.  
21 doi:10.1016/0924-977x(91)90004-e
- 22 98. Olson ME, Eubanks LM, Janda KD. Chemical Interventions for the Opioid Crisis: Key  
23 Advances and Remaining Challenges. *J Am Chem Soc.* 2019;141(5):1798-1806.  
24 doi:10.1021/jacs.8b09756
- 25 99. Lynch G, Gall CM. Ampakines and the threefold path to cognitive enhancement. *Trends*  
26 *Neurosci.* 2006;29(10):554-562. doi:10.1016/j.tins.2006.07.007
- 27 100. Yuan CL, Shi EY, Srinivasan J, Ptak CP, Oswald RE, Nowak LM. Modulation of AMPA  
28 Receptor Gating by the Anticonvulsant Drug, Perampanel. *ACS Med Chem Lett.*  
29 2019;10(3):237-242. doi:10.1021/acsmchemlett.8b00322

- 1 101. Potschka H, Trinka E. Perampanel: Does it have broad-spectrum potential? *Epilepsia*.  
2 2019;60 Suppl 1:22-36. doi:10.1111/epi.14456
- 3 102. Coombs ID, Ziobro J, Krotov V, Surtees TL, Cull-Candy SG, Farrant M. A gain-of-  
4 function GRIA2 variant associated with neurodevelopmental delay and seizures: Functional  
5 characterization and targeted treatment. *Epilepsia*. 2022;63(12):e156-e163.  
6 doi:10.1111/epi.17419
- 7 103. Jackson AC, Nicoll RA. The expanding social network of ionotropic glutamate receptors:  
8 TARPs and other transmembrane auxiliary subunits. *Neuron*. 2011;70(2):178-199.  
9 doi:10.1016/j.neuron.2011.04.007
- 10 104. Schwenk J, Fakler B. Building of AMPA-type glutamate receptors in the endoplasmic  
11 reticulum and its implication for excitatory neurotransmission. *J Physiol*.  
12 2021;599(10):2639-2653. doi:10.1113/JP279025
- 13 105. Silk M, Petrovski S, Ascher DB. MTR-Viewer: identifying regions within genes under  
14 purifying selection. *Nucleic Acids Res*. 2019;47(W1):W121-W126. doi:10.1093/nar/gkz457

## 16 **Figure legends**

17 **Figure 1 Location of *GRIA3* variants in the GluA3 receptor and effect on glutamate-gated**  
18 **channel function.** (A) Structural model of homomeric GluA3 receptor encoded by the *GRIA3*  
19 gene built from structures of the GluA2 receptor (*Supplementary materials & methods*). The top  
20 left panel shows a surface representation of the tetrameric receptor complex with the four  
21 identical subunits in shades of gray and blue. The bottom panel shows a cartoon representation of  
22 a single GluA3 subunit with the N-terminal domain (NTD) in light blue, the agonist-binding  
23 domain (ABD) in blue, and the transmembrane domain (TMD) in magenta. Zoomed views of the  
24 NTD, ABD, and TMD shows the position of genetic variants caused by *GRIA3* missense variants  
25 highlighted by different colors according to the apparent effect on homomeric GluA3 function as  
26 neutral (*gray*), LoF (*red*), and GoF (*green*). Orange circle indicate the position of the Glu binding  
27 site in the LBD. (B) Summary of desensitized (Glu) and non-desensitized (Glu+CTZ) current  
28 amplitudes and Glu EC50 for homomeric GluA3 receptors containing genetic variants encoded

1 by the *GRIA3* variants evaluated in this study. Values, number of measurements, and statistical  
2 parameters are given in Tables S2 and S3. Individual data points are color-coded according to the  
3 effect on currents or EC50 (LoF effect; *red*) or increase (GoF effect; *green*). For the EC50 panel,  
4 data points shown as squares represent EC50 values determined with CTZ. (C) Representative  
5 current responses from TEVC recordings of XO ( $V_{\text{HOLD}} -40$  mV) expressing WT or *GRIA3*  
6 variant-containing GluA3 receptors in response to Glu application ( $300 \mu\text{M}$ , *black bar*) in the  
7 presence of CTZ ( $100 \mu\text{M}$ ) to block desensitization. (D) Representative current recordings from  
8 TEVC Glu concentration-response experiments of WT GluA3 and selected variants  
9 exemplifying neutral (p.(Ala615Val)), increasing (p.(Ala654Val)), or decreasing  
10 (p.(Thr776Met)) effect on receptor responsiveness to Glu. (E) Composite concentration-response  
11 curves for WT and selected *GRIA3* variant-containing GluA3 receptors. Data points represent the  
12 mean of 6 to 12 oocytes. Error bars are the SEM and are shown when larger than the symbol  
13 size. The current responses are normalized to the maximal response evoked by Glu. In all panels,  
14 variants are labelled with single-letter amino acid codes.

15

16 **Figure 2 Variant effects on receptor desensitization and activation properties.** (A)  
17 Representative currents evoked by sequential 10-20 s applications of Glu ( $1 \text{ mM}$ , *black bar*)  
18 alone and in the presence of CTZ ( $100 \mu\text{M}$ , *gray bar*) from oocytes expressing WT GluA3 and  
19 GluA3 carrying selected *GRIA3* missense variants. The p.(Pro302Ser) variant shows no change  
20 in the size of the desensitized current relative to the non-desensitized Glu current compared to  
21 WT, the p.(Ala654Val) variant shows increased desensitized current, and the p.(Thr816Ile)  
22 variant show decreased desensitized current. (B) Representative currents evoked by sequential  
23 10-20 s applications of Glu ( $1 \text{ mM}$ , *black bar*) and KA ( $300 \mu\text{M}$ ; *blue bars*) in the presence of  
24 CTZ ( $100 \mu\text{M}$ , *gray bar*) from oocytes expressing WT GluA3 and GluA3 containing selected  
25 variants exemplifying different types of variant effects on KA/GLU response ratio. For WT  
26 GluA3 and the p.(Pro302Ser) variant, the KA-evoked current has an amplitude of 16% of the  
27 Glu current amplitude. In contrast, the p.(Ala654Val) variant has a relative KA current of 41%,  
28 indicating an increase in activation properties, and p.(Ala653Thr) variant has decreased relative  
29 KA response amplitude of 3.5%, indicating decreased activation properties. The holding  
30 potential was  $-40$  mV in all shown recordings. (C) Representative currents illustrating NASPM  
31 ( $1 \mu\text{M}$ , *red bar*) inhibition of Glu evoked currents for WT GluA3 and GluA3 containing the

1 variants p.(Arg631Ser) and p.(Ala654Pro) **(D)** Summary of the ratio of desensitized and non-  
2 desensitized current amplitude ( $I_{\text{Glu}}/I_{\text{Glu+CTZ}}$ ), non-desensitized Glu and KA ( $I_{\text{KA+CTZ}}/I_{\text{Glu+CTZ}}$ )  
3 current amplitudes and NASPM inhibition of Glu-evoked current for homomeric GluA3  
4 receptors containing genetic variants encoded by the *GRIA3* variants evaluated in this study.  
5 Values, number of measurements, and statistical parameters are given in Table S2. Individual  
6 data points are color-coded according to the effect on currents or  $EC_{50}$  (LoF effect; *red*) or  
7 increase (GoF effect; *green*). **(E-G)** Summary of phenotype and domain location of variants with  
8 overall GoF (E), LoF (F), and neutral (G) effect on homomeric GluA3 receptor function.  
9 Symbols indicate: ▼; decrease, ▲; increase, ●; no change, -; not determined. Color coding  
10 indicates a predicted LoF (*red*) or GoF (*green*) effect of change on overall receptor function. **(H)**  
11 Missense tolerance ratio (MTR) of *GRIA3* variants analyzed with a 31 amino acid window  
12 calculated using the MTR-viewer online tool (<https://biosig.lab.uq.edu.au/mtr-viewer/>)<sup>105</sup>. A line  
13 graph displays the MTR distribution for *GRIA3* (gene transcript NM\_000828) with regions in  
14 orange indicating observed variation differs significantly from neutrality. Dashed lines on the  
15 plot denote gene-specific MTRs: green = 5th percentile, purple = 25th percentile and black =  
16 50th percentile. Above the MTR distribution is shown the domain structure of the GluA3  
17 subunit. Variant positions are shown as circles on the MTR line graph and colored according to  
18 functional effect as: neutral (*gray*), GoF (*green*), and LoF (*red*). Orange line segments indicate  
19 regions where the observed variation differs significantly from neutrality. In all panels, variants  
20 are labelled with single-letter amino acid codes.

21  
22 **Figure 3 Variant effects in heteromeric GluA2/A3 receptors.** **(A)** Representative currents  
23 evoked by sequential 10-20 s applications of Glu (1 mM, *black bar*) alone and in the presence of  
24 CTZ (100  $\mu\text{M}$ , *gray bar*) from oocytes expressing WT GluA2 and WT GluA3 and WT GluA2  
25 with GluA3 carrying selected *GRIA3* missense variants illustrating increased (p.(Ala654Val),  
26 *middle trace*) and decreased (p.(Leu774Ser); *lower trace*) desensitized current. **(B)**  
27 Representative currents evoked by sequential 10-20 s applications of Glu (1 mM, *black bar*) and  
28 KA (300  $\mu\text{M}$ ; *blue bars*) the presence of CTZ (100  $\mu\text{M}$ , *gray bar*) from oocytes expressing WT  
29 GluA2 and WT GluA3 and WT GluA2 with GluA3 carrying selected *GRIA3* missense variants  
30 illustrating increased (p.(Ala615Val), *middle trace*) and decreased (p.(Ala653Thr); *lower trace*)  
31 current response to KA relative to Glu. **(C)** Representative current recordings from TEVC Glu

1 concentration-response experiments of WT and selected variants in heteromeric GluA2/A3  
2 receptors with corresponding fitted dose-response curves for homomeric (A3) and heteromeric  
3 (A2/A3) receptors. The p.(Trp799Leu) exemplifies a variant changing the EC<sub>50</sub> in both  
4 homomeric and heteromeric receptors, whereas p.(Thr776Met) exemplifies a variant affecting  
5 only homomeric receptors. Color code of curves indicate effect on EC<sub>50</sub>: Decrease (*green*),  
6 increase (*red*), or neutral (*gray*). **(D)** Overview and summary of the effects on heteromeric  
7 GluA2/A3 receptor parameters (*squares*) of *GRIA3* variants with GoF (*green*) and LoF (*red*)  
8 effects. Data points represent the mean and 95% CI values (see Supplementary Tables S2 and  
9 S3). **(E)** IV relationships of Glu-evoked currents from oocytes expressing homomeric WT and  
10 variant-containing GluA3 alone (*white circles*) and with WT GluA2R (*black circles*). The  
11 current amplitude at the different holding potentials is normalized to the current at -40 mV. Data  
12 points represent the mean from 6 to 10 oocytes. Error bars indicate the SEM and are shown when  
13 larger than the symbol size. In all panels, variants are labelled with single-letter amino acid  
14 codes.

15  
16 **Figure 4 Characterization of variant effect on fast receptor kinetics.** **(A)** Representative  
17 whole-cell currents evoked by a 500 ms application of Glu (10 mM, *black bar*) from homomeric  
18 GluA3 (*left*) and heteromeric GluA2/A3 receptors carrying the indicated *GRIA3* variants  
19 subunits expressed in HEK293 cells. The holding potential was -70 mV in all recordings. Note  
20 that scale bars for current amplitude differ between recordings. **(B)** The time constant ( $\tau_{des}$ ) and  
21 level ( $I_{ss}$ ) of current desensitization determined from the fitting of the current decay (*insert*)  
22 during 500 ms applications of Glu (10 mM, *black bars*) fitted to two-exponential decay functions  
23 weighted by proportional contributions for WT and variant homomeric GluA3 (*left*) and  
24 heteromeric GluA2/A3 (*right*) receptors. **(C)** Summary of the  $\tau_{des}$  and  $I_{ss}$  values. Bars represent  
25 the mean with SEM error. Values not determined due to low or no current are labelled *nd*. **(D)**  
26 Deactivation rates ( $\tau_{deact}$ ) determined from the fitting of the current decay (*insert*) following 1 ms  
27 application of Glu (10 mM, *black bars*) fitted to a mono-exponential decay function (*inserts*) for  
28 WT and variant homomeric GluA3 (*left*) and heteromeric GluA2/A3 (*right*) receptors. **(E)**  
29 Summary of  $\tau_{deact}$  values. Bars represent the mean with SEM error. Values not determined due to  
30 low or no current are labelled *nd*. **(F)** Summary of effects of patient variants on current kinetics  
31 and location in GluA3 subunit. Variants with LoF effects are shown in red and GoF in green. ▼;

1 decrease, ▲; increase, ●; no change, -; not determined. In all panels, variants are labelled with  
 2 single-letter amino acid codes.

3

4 **Figure 5 Variant classification and phenotype correlations for patient M1-M12 and F1-F10.**

5 (A) Schematic overview of the classification of receptor phenotype for patients M1-M13 and F1-  
 6 F11 into severe and mild GoF (*green*) and LoF (*red*) categories based on variant effect patterns  
 7 on GluA3-containing receptor function together with an overview of the number of patients and  
 8 prevalence of key patient symptoms for each category. (B) Summary of key and supporting  
 9 features for the clinical phenotypes associated with LoF and GoF variants. The diagram  
 10 summarizes several clinical findings that can help predict if a *GRIA3* variant leads to loss-of-  
 11 function (LoF) and gain-of-function (GoF). GoF variants manifest with seizures occurring before  
 12 the first year of life (with a median age of 1 month) and are characterized by supporting features  
 13 such as hypertonia, hyperekplexia/excessive startle reflex, and the absence of sleep disturbances.  
 14 LoF variants manifest with key features such as seizure onset after the first year of life (with a  
 15 median age of 16 months) and supporting features including hypotonia, sleep disturbances, and  
 16 the absence of hyperekplexia/excessive startle reflex. If a patient's phenotypical presentation  
 17 displays a combination of these features, functional testing of the variant is required to determine  
 18 whether a *GRIA3* variant displays LoF or GoF characteristics. <sup>a-d</sup> *P* values for comparing  
 19 proportions of clinical indicators between the LoF or GoF patients: <sup>a</sup> Age of seizure onset < 12  
 20 months versus age of seizure onset > 12 months; *P* = 0.004, <sup>b</sup> hypertonia versus hypotonia; *P* =  
 21 0.0004, <sup>c</sup> hyperekplexia/startle versus no hyperekplexia/startle; *P* = 0.003, <sup>d</sup> sleep disturbance  
 22 versus no sleep disturbance; *P* = 0.018.

23

24 **Table I Comparison of clinical features reported in patients with loss-of-function *GRIA3* variants compared to features**  
 25 **reported in those with gain-of-function *GRIA3* variants**

Feature	Loss-of-function	Gain-of-function
Number of patients	15	10
Male	12/15 (80%)	2/10 (20%)
Female	3/15 (20%)	8/10 (80%)
Epilepsy diagnosis	5/15 (33%)	6/10 (60%)
Median age at onset of seizures	16 months (range 9 mo to 3 yrs)	1 month (range 1 <sup>st</sup> day to 27 yrs)
Treatment resistant seizures	3/5 (60%)	4/6 (66%)
Developmental delay or cognitive impairment	15/15 (100%)	10/10 (100%)

	Degree: borderline = 1 mild-moderate = 1 moderate = 4 severe = 7 severe-profound = 1 profound = 1	Degree: moderate = 4 severe = 2 severe-profound = 1 profound = 3
Muscular hypotonia	12/15 (80%)	0/10 (0%)
Muscular hypertonia	2/15 (13%)	9/10 (90%)
Hyporeflexia	10/15 (66%)	0/10 (0%)
Hyperreflexes	1/15 (6%)	7/10 (70%)
Spasticity	1/15 (6%)	4/10 (40%)
Movement disorder or any kind	7/15 (46%)	8/10 (80%)
Hyperexplexia or stimulus sensitive non-epilepticus myoclonia	2/15 (13%)	6/10 (60%)
Sleep disorder	10/15 (66%)	3/10 (33%)
Behavioral issues of any kind	10/15 (66%)	5/10 (50%)
Aggressive outburst or self-damaging behavior	6/15 (40%)	2/10 (20%)
Magnetic resonance imaging (MRI) performed	9/15 (60%)	9/10 (90%)
Abnormal MRI	2/9 (22%)	2/9 (22%)

1 The table summarizes key clinical features in the loss-of-function and gain-of-function patient groups. Detailed clinical information for individual  
2 patients is provided in Supplementary Information and Table S7.

ACCEPTED MANUSCRIPT





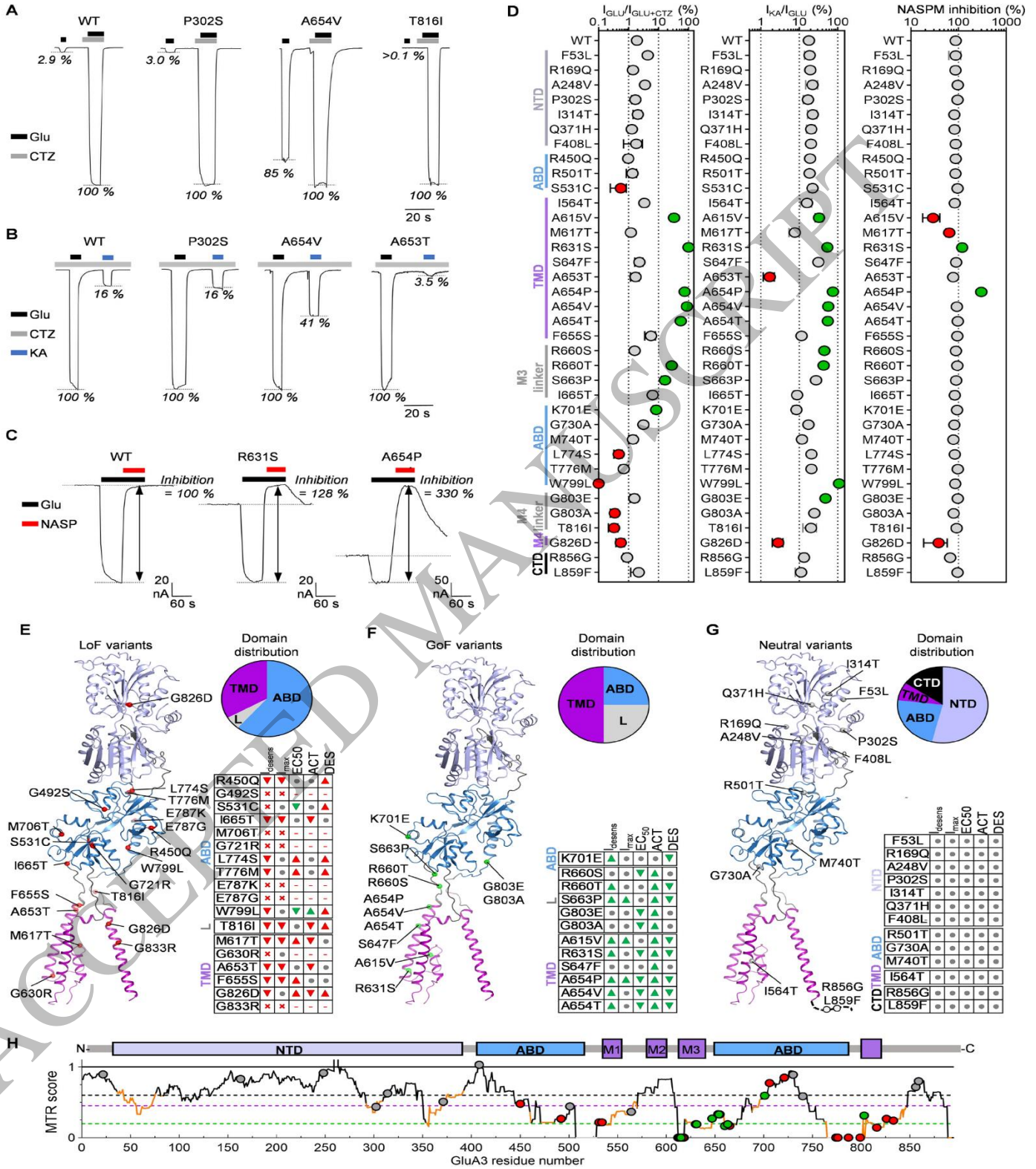


Figure 2  
185x247 mm (x DPI)

1  
2  
3  
4

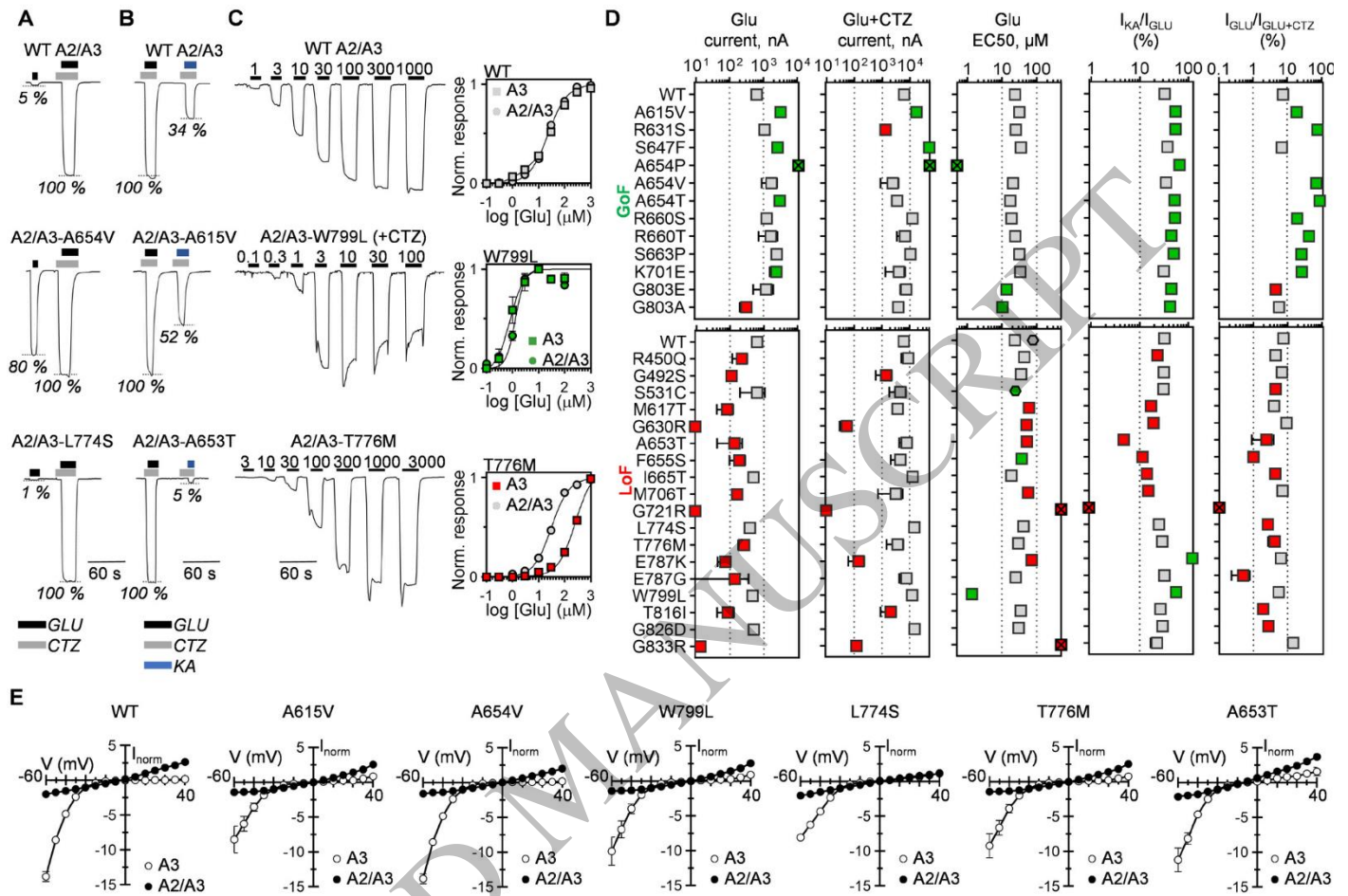


Figure 3  
185x127 mm (x DPI)

1  
2  
3  
4

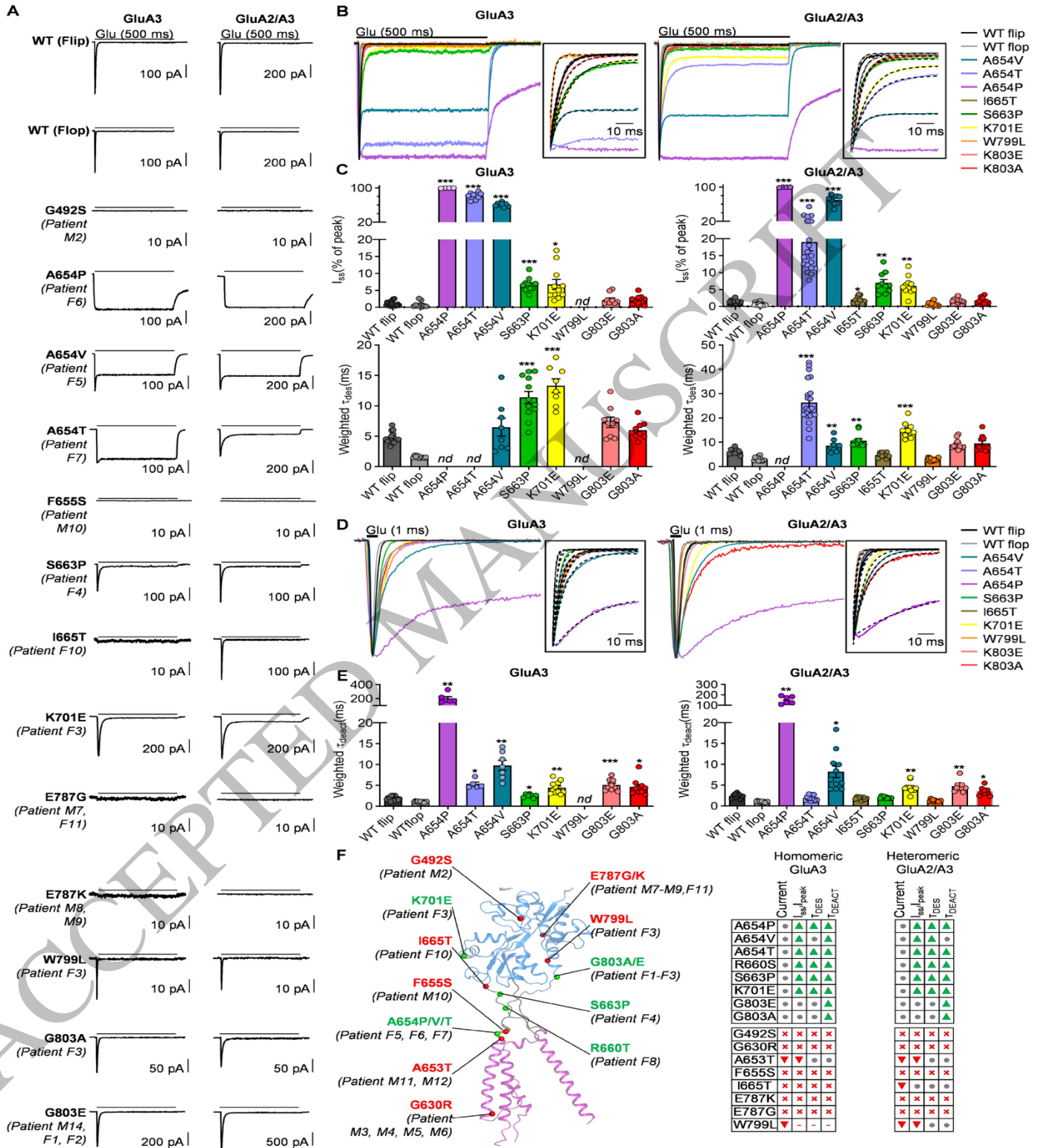


Figure 4  
185x247 mm ( x DPI)

1  
2  
3  
4

A

	Female patients (variant)		Male patients (variant)		
	F10(I665T)	F11(E787G)	F3(W799L)	F1-F2(G803E)	F4(S663P) F5(A654V) F6(A654P) F7(A654T) F8(R660T) F3(K701E)
	M1(Q371fs)	M2(G492S)	M3-6(G630R)	M10(F655S)	
	M7(E787G)	M8-9(E787K)	M11-M12(A653T)	M14(G803E)	M13(G803A)
	<b>LoF</b>	<b>Severe</b>	<b>Mild</b>	<b>Mild</b>	<b>Severe</b> <b>GoF</b>
Receptor phenotype	Peak current	complete loss	decreased	no change	increased/no change
	Steady-state current	complete loss	decreased	no change	increased
	Activation	-	decreased	increased	increased
	Desensitization	-	increased/no change	decreased	blocked/decreased
	Deactivation	-	unknown/no change	slowed	slowed
	Glu sensitivity	-	increased/no change	increased	increased
Clinical phenotype	Hypotonia	9(12)	3(3)	0(4)	0(6)
	Hypertonia	1(12)	0(3)	4(4)	6(6)
	Hyperekplexia	0(12)	0(3)	1(4)	4(6)
	Sleep disturbance	7(12)	3(3)	1(4)	2(6)

B

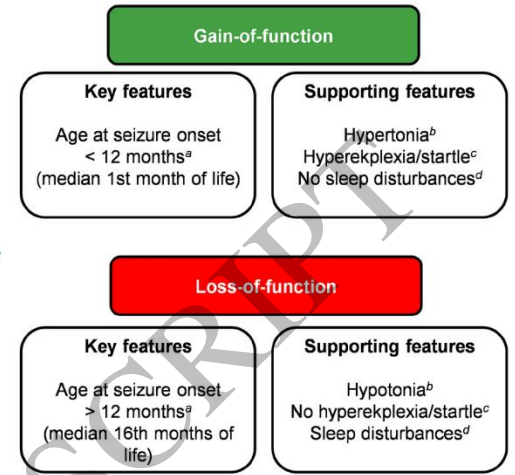


Figure 5  
177x80 mm ( x DPI)

1  
2  
3

ACCEPTED MANUSCRIPT